Rita de Sá Martins Pinto Gonçalves

Licenciatura em Biologia pela Faculdade de Ciências da Universidade de Lisboa

Study of *in vivo* interactions between penicillin-binding proteins of *Staphylococcus aureus*

Dissertação para obtenção do Grau de Mestre em Genética Molecular e Biomedicina da FCT/UNL

Orientador: Mariana Gomes de Pinho, Professora Associada
Instituto de Tecnologia Química e Biológica/ UNL

Júri:

Presidente: Prof.ª Dr.ª Ilda Santos Sanches
Arguente: Prof. Dr. Luís Jaime Mota
Vogal: Prof.ª Dr.ª Mariana Gomes de Pinho

FACULDADE DE CIÊNCIAS E TECNOLOGIA
UNIVERSIDADE NOVA DE LISBOA

Setembro 2015

Rita de Sá Martins Pinto Gonçalves

Licenciatura em Biologia pela Faculdade de Ciências da Universidade de Lisboa

Study of *in vivo* interactions between penicillin-binding proteins of *Staphylococcus aureus*

Dissertação para obtenção do Grau de Mestre em Genética Molecular e Biomedicina da FCT/UNL

Orientador: Mariana Gomes de Pinho, Professora Associada
Instituto de Tecnologia Química e Biológica/ UNL

Júri:

Presidente: Prof.ª Dr.ª Ilda Santos Sanches
Arguente: Prof. Dr. Luís Jaime Mota
Vogal: Prof.ª Dr.ª Mariana Gomes de Pinho

FACULDADE DE CIÊNCIAS E TECNOLOGIA
UNIVERSIDADE NOVA DE LISBOA

Setembro 2015

Study of *in vivo* interactions between penicillin-binding proteins of *Staphylococcus aureus*

ACKNOWLEDGMENTS

I would like to sincerely thank Dra. Mariana Pinho, my supervisor, for the opportunity to integrate the Bacterial Cell Biology team at the ITQB and develop this challenging work. For being a great mentor throughout this year, for the helpful discussions, knowledge and guidance she gave me to develop my capacities in the laboratory and dedicate myself despite of any obstacle. To Nathalie, for her guidance and help in the beginning of this work, for pushing me harder to achieve my goals and realize that for a big project time is always never too much. I truly thank her for providing me final strain needed to complete this work. A special thanks to my dear colleagues, Pedro, Raquel, Teresa and Vanessa for the great knowledge and help they gave me throughout this work. Teresa and Vanessa, colleagues and friends, for fulfilling my days with joy. Helena and Trish, for sharing their wise ideas and for contributing for a great work environment. Finally, but not least, to my family; mother, father, brothers and grandmother, for the constant support and motivation. Without all of them I would have not been able to develop my ideas during this demanding year and, most of all, to grow academically and personally.

RESUMO

Staphylococcus aureus (S. aureus) é um organismo patogénico humano de grande relevância que adquiriu resistência a praticamente todas as classes de antibióticos, sendo responsável por um elevado número de infeções resistentes principalmente a antibióticos β-lactâmicos a nível hospitalar e comunitário. Os β-lactâmicos têm como alvo as proteínas de ligação à penicilina (PBPs) e estas são responsáveis por catalisar os últimos estágios de síntese do principal componente da parede celular, o peptidoglicano. Tal como em *Escherichia coli,* foi sugerido que *S. aureus* sintetiza a parede celular através de um complexo multi-proteico. Na presença de β-lactâmicos, as proteínas PBP2A e PBP2 sintetizam a parede celular, garantindo a sobrevivência celular. A PBP2 coopera com a PBP4 nas para estabelecer as ligações peptidicas entre os polímeros da parede celular. Como tal, a investigação da interação entre estas proteínas e a sua localização *in vivo* é de grande interesse, pois fornece novas pistas acerca da maquinaria de síntese da parede celular em *S. aureus.* O objetivo deste trabalho foi desenvolver um sistema de Split-GFP_{P7} para determinar as interações entre a PBP2 e a PBP4. Dividiu-se o GFP_{P7} num local estratégico e fizeram-se fusões de proteínas de interesse a ambas as porções resultantes. Quando se expressou uma fusão contendo o fragmento de GFP_{P7} ligado a determinada proteína, não foi detetada fluorescência na célula. Pelo contrário, quando ambos os fragmentos de GFP_{P7} em fusão com proteínas de síntese do peptidoglicano (PBP2 e PBP4) ou de divisão celular (FtsZ e EzrA) foram expressos na mesma célula, detetou-se fluorescência celular a nível do septo. Contudo, análises posteriores revelaram que este resultado se deve à auto-associação do GFP_{P7}. Deste modo, interpretamos os resultados com base neste acontecimento e fornecemos novas pistas que possam ser úteis para o melhoramento deste sistema.

Palavras-chave: *Staphylococcus aureus*, síntese do peptidoglicano, proteínas de ligação à penicilina (PBPs), PBP2, PBP4, sistema de Split-GFP_{P7}

ABSTRACT

Staphylococcus aureus (*S. aureus*) is a major human pathogen that has acquired resistance to practically all classes of β-lactam antibiotics, being responsible of Multidrug resistant *S. aureus* (MRSA) associated infections both in healthcare (HA-MRSA) and community settings (CA-MRSA). The emergence of laboratory strains with high-resistance (VRSA) to the last resort antibiotic, vancomycin, is a warning of what is to come in clinical strains. Penicillin binding proteins (PBPs) target β-lactams and are responsible for catalyzing the last steps of synthesis of the main component of cell wall, peptidoglycan. As in *Escherichia coli*, it is suggested that *S. aureus* uses a multi-protein complex that carries out cell wall synthesis. In the presence of β-lactams, PBP2A and PBP2 perform a joint action to build the cell wall and allow cell survival. Likewise, PBP2 cooperates with PBP4 in cell wall cross-linking. However, an actual interaction between PBP2 and PBP4 and the location of such interaction has not yet been determined. Therefore, investigation of the existence of a PBP2-PBP4 interaction and its location(s) *in vivo* is of great interest, as it should provide new insights into the function of the cell wall synthesis machinery in *S. aureus*. The aim of this work was to develop Split-GFP_{P7} system to determine interactions between PBP2 and PBP4. GFP_{P7} was split in a strategic site and fused to proteins of interest. When each GFP_{P7} fragment, fused to proteins, was expressed alone in staphylococcal cells, no fluorescence was detectable. When GFP_{P7} fragments fused to different peptidoglycan synthesis (PBP2 and PBP4) or cell division (FtsZ and EzrA) proteins were co-expressed together, fluorescent fusions were localized to the septum. However, further analysis revealed that this positive result is mediated by GFP_{P7} self-association. We then interpret the results in light of such event and provide insights into ways of improving this system.

Keywords: *Staphylococcus aureus;* MRSA, Peptidoglycan synthesis, Penicillin-binding proteins 2 and 4, Split-GFP_{P7} system

TABLE OF CONTENTS

FIGURES AND TABLES INDEX

SYMBOLS AND ABBREVIATIONS

%	Percentage
°C	Degrees Celsius
~	Approximately
Amp	Ampicillin
B. subtilis	*Bacillus subtilis*
BTH	Bacterial two-hybrid
bp	Base pair
BiFC	Bimolecular fluorescence complementation assay
$CdCl_2$	Cadmium Chloride
Cm	Chloramphenicol
DNA	Deoxyribonucleic acid
DNAse	Deoxyribonuclease
dNTP	Deoxyribonuclotide triphosphate
E. coli	*Escherichia coli*
EDTA	Ethylenediaminetetraacetic acid
Erm	Erythromycin
eYFP	Enhanced yellow fluorescent protein
FastAP	Thermosensitive Alkaline Phosphatase
FP(s)	Fluorescent protein(s)
GFP	Green fluorescent protein
GFP_{P7}	Superfast green fluorescent protein
h	Hour(s)
IPTG	Isopropyl β-D-thiogalactosidase
KAc	Potassium acetate
Kan	Kanamycin
kb	Kilo base pair
LA	Luria-Bertani agar
LB	Luria-Bertani broth
M	Molar
min	Minute(s)
$MnCl_2 \cdot 4H_2O$	Manganese(II) chloride tetrahydrate
MOPS	3-(*N*-morpholino)propanesulfonic acid
MRSA	Methicilin-resistant *Staphylococcus aureus*
MSSA	Methicilin-sensitive *Staphylococcus aureus*
NaCl	Sodium chloride
Neo	Neomycin
OD_{600}	Optical density at 600 nm
PBP(s)	Penicillin-binding protein(s)
PCR	Polymerase chain reaction
PG	Peptidoglycan
$RbCl_2$	Rubidium Chloride
Rpm	Revolutions per minute
S. aureus	*Staphylococcus aureus*
TPase	Transpeptidase
TGase	Transglycosylase
TSA	Tryptic soy agar
TSB	Tryptic soy broth

VISA	Vancomycin-intermediate *Staphylococcus aureus*
VRSA	Vancomycin-resistant *Staphylococcus aureus*
WT	Wild-type
WTA	Wall teichoic acid(s)
X-Gal	5-bromo-4-chloro-3-indolyl-β-D-galactopyranoside
Xyl	Xylose

INTRODUCTION

1.1 *Staphylococcus aureus*: Importance as a pathogen

Staphylococcus aureus is a prominent pathogen well known for its virulence and antibiotic resistance in both community and nosocomial settings. Virulence is mediated by innumerous factors, such as secreted or cell surface-associated proteins that compromise the host immune system to help colonization (Foster, 2005). The major importance of this pathogen increased with the development of resistance to most classes of antibiotics.

Penicillin was an effective antimicrobial agent that protected against *S. aureus* infections. Soon after the first use of penicillin in 1942 in the U.S, penicillinase-producing *S. aureus* emerged in the clinical setting and its prevalence increased dramatically within a few years, mostly due to wide use of penicillin. Since then, Penicillin-resistant *S. aureus* (PRSA), phage-type 80/81 *clone*, become pandemic and in the late 1950s, a new antibiotic, methicillin, was used to select against PRSA strains. Shortly after the introduction of methicillin, in 1961, the first cases of methicillin- resistant *S. aureus* (MRSA) strains were reported. MRSA emerged in the U.S in the early 1960s and have since spread among hospital and health care settings worldwide (Deleo and Chambers, 2009). More recently, in the 1990s, MRSA strains have spread into the community, among healthy individuals, giving rise to new epidemic waves of community acquired *S. aureus* (CA-MRSA) (Udo *et al*., 1993; Deleo and Chambers, 2009). MRSA is resistant to practically all available β-lactams, which include penicillin, amoxicillin, oxacillin, methicillin, and others (Deleo and Chambers, 2009).

The mechanism of β-lactam resistance involves the acquisition of *mecA* gene, which encodes for a protein, penicillin-binding protein 2A (PBP2A), which, unlike other staphylococcal PBPs, has low affinity for ß-lactam antibiotics (Fuda *et al*., 2005). This methicillin resistance gene, *mecA* gene, has evolved from a frequent skin colonizer of animals, *Staphylococcus sciuri*, and is included in staphylococcal chromosome cassette *mec* (SCC*mec*), a mobile genetic element which is horizontally transferable among staphylococcal species (Katayama *et al*., 2000; Katayama *et al*., 2003). Until 2009, only five distinct staphylococcal cassette chromosome mec (SCCmec) types were identified in MRSA strains. However, eleven different SSCmec types have been described to date in *S. aureus*, reflecting the rate of MRSA evolution (Deleo and Chambers, 2009; Shore and Coleman, 2013). Health care–associated MRSA (HA-MRSA) and community acquired MRSA (CA-MRSA) strains differ in their genetic background: HA-MRSA contain mainly SCCmecI–III, whereas CA-MRSA frequently carries SCCmecIV (Okuma *et al*., 2002; de Lencastre *et al*., 2007). Moreover, CA-MRSA shows higher virulence than HA-MRSA in a mouse model of *S. aureus* infection

(Voyich *et al*., 2005). These strains express Panton-Valentine leukocidin (PVL) toxin, which is often used as a marker for CA-MRSA. (Wardenburg *et al*., 2009).

Vancomycin is a glycopeptide antibiotic used as an alternative to β-lactams for treatment of MRSA infections as it inhibits synthesis of *S. aureus* cell wall by a different mechanism from these antibiotics (Walsh and Howe 2002). However, according to some authors, it showed reduced efficacy due to weak antimicrobial activity and poor tissue penetration comparing to other β-lactams. The poor therapeutic effect along with the rapid reduction of *S. aureus* susceptibility to vancomycin has led to questioning its effectiveness in the long run (Deresinski, 2007). After the first clinical isolate of MRSA *S. aureus* with decreased susceptibility to vancomycin, vancomycin-intermediate *S. aureus* (VISA) strains spread across several countries (Howe *et al*., 2004). A thickened cell wall contributes to the vancomycin resistance and is a common phenotype in these isolates (Cui *et al*., 2000). This altered composition is related to a decrease in highly cross-linked muropeptides that compose the PG, along with an increase in muropeptides monomers and dimers (Sieradzki and Tomasz, 1997; Sieradzki *et al*., 1999), which is in turn associated to defects in penicillin-binding protein 4 (PBP4) activity (Sieradzki *et al*., 1999). A few years later, strains highly resistant to vancomycin, designated vancomycin-resistant *S. aureus* (VRSA) have emerged and vancomycin efficacy as an antistaphylococcal antibiotic is threatened (Bartley, 2002; Deresinski, 2007).

1.2 Mechanisms of Cell Growth in bacteria

Cell division and cell wall synthesis are two essential processes for bacterial growth that are carried out by multiprotein complexes. *Escherichia coli* (*E. coli*) and *Bacillus subtilis* (*B. subtilis*) are rod-shape bacteria which have been used as model organisms to understand the mechanisms of cell division, namely the localization and order by which proteins are recruited to the division site (reviewed in Errington *et al*., 2003)

1.2.1 Cell Division

Cell division or cytokinesis in bacteria is accomplished by a macromolecular machine, known as the divisome, which involves an organized targeting of multiple proteins to the site of division. (Errington *et al*., 2003). Cell division begins with the formation of a Z-ring at the mid-cell, which is spatial and temporally regulated by two different mechanisms, the Min system and nucleoid occlusion (NO) (Bi and Lutkenhaus, 1991; Errington *et al*., 2003). FtsZ is a highly conserved tubulin homologue and a key component for initiation of the Z-ring assembly (Erickson, 1997; Adams and Errington 2009). FtsZ is initially recruited to form a ring structure (Z-ring) and polymerization of filaments depends on its GTPase activity (Lutkenhaus

and Addinall, 1997). The Z-ring serves as scaffold for the recruitment of later divisome proteins and directs synthesis, location and shape of the division septum. *B. subtilis* and *E. coli* are rod-shaped bacteria frequently used as model organisms to study the mechanisms of cell division. In these bacteria, the site of division is the mid-cell. *B. subtilis* and *E. coli* divide through a medial plane. Unlike these bacteria, coccoid shaped bacteria *S. aureus* divides by three perpendicular planes in 3 phases of the cell cycle (Pinho *et al*. 2013).

In *E. coli* several proteins are involved in assembly of Z-ring. The divisome components target the division site in a co-ordinate manner to form the septal Z-ring (Errington *et al*., 2003; Weiss, 2004). FtsZ filaments tethering to the membrane involves two proteins, FtsA and ZipA, which bind to its short highly conserved C-tail. These proteins are composed by a transmembrane domain and a cytoplasmic domain that are connected by a flexible linker (Pichoff *et al*, 2012). It has been shown that either FtsA or ZipA is required to form and stabilize the preformed Z-rings (Pichoff and Lutkenhaus 2002). Importantly, FtsA location to the division site is needed for recruitment of the later-assembling membrane-bound division proteins. Therefore, recruitment of nine essential proteins, designated Fts proteins (FtsE/X, FtsK, FtsQ/L/B, FtsW/I) and PBP1b to the divisome is dependent on the amount of monomeric FtsA at the Z ring. Fts proteins assemble to the Z-ring in a defined order, which is still not well known. Non-essential proteins ZapA-D are then recruited to the Z ring to promote its integrity (Lutkenhaus *et al*., 2012). It is suggested that septal synthesis is activated when PBP3 is recruited to the septum by the lipid II flippase FtsW to interact with the ternary FtsQLB complex, PBP1B and FtsN. FtsN is an essential protein that triggers septation. AmiB and AmiC hydrolases are recruited by EnvC and NlpD respectively, participate in splitting of the septum to separate daughter cells. The Tol-Pal complex enables invagination of the outer membrane, to finally drive cell separation (Buddelmeijer and Beckwith, 2004; Typas *et al*., 2012; Lutkenhaus *et al*., 2012).

In *B. subtilis*, as in *E.coli*, the Z-ring assembles to form a septum at the mid-cell site that constricts and culminates with cell division, giving rise to two cells of the same size. Likewise, *B. subtilis* divisome includes multiple proteins that directly participate in septum formation. In an early stage of divisome assembly, four proteins (FtsA, EzrA, ZapA and SepF) are recruited in an independent manner to bind directly with FstZ **(Fig.1.1).** These proteins play different roles in cell division. FtsA is important for the attachment of the Z-ring to the membrane and is probably required for the assembly of the later components of the divisome onto the Z-ring. ZapA, stabilizes the Z-ring, promoting bundling of FtsZ protofilaments. EzrA and SepF play regulatory and/or structural roles in FtsZ polymerization. After assembly of the early divisome proteins onto the Z-ring, seven divisome proteins (DivIB, DivIC, FtsW, FtsL, PBP2B, GspB, PBP1) are recruited to that location. Their recruitment must depend on the interaction with FtsZ-binding proteins, as they apparently do not bind directly to FtsZ. These proteins are bound to the membrane and contain large periplasmic domains that suggest a role in septal peptidoglycan (PG) assembly (Graumman,

2012a). Unlike *E. coli*, later divisome proteins are targeted to the division site, in an interdependent manner (Errington et al., 2003). DivIB, DivIC and FtsL have similar structures and are likely to interact to form a ternary complex (DivIB-DivIC-FtsL), which is equivalent to the FtsQLB complex in *E. coli*. It has been proposed that within this subcomplex, DivIC interacts with FtsL and DivIB binds to the DivIC-FtsL heterodimer. PBP2B is then recruited, binds to DivIB and directs the PG synthesis machinery to the division site (Graumman, 2012a). It is suggested that the DivIB-DivIC-FtsL trimeric complex may have a role in PG metabolism at the septum through interactions with PBP2B (Rowland *et al*., 2010). Although it is not well known which proteins are involved in PBP1 late recruitment to the divisome, some authors suggest dependence on DivIB, DivIC, and PBP2B (Scheffers and Errington, 2004), while others defend that GspB/YspB complex acts together with EzrA to shuttle PBP1 to the divisome (Claessen *et al*., 2008; Tavares *et al*., 2008).

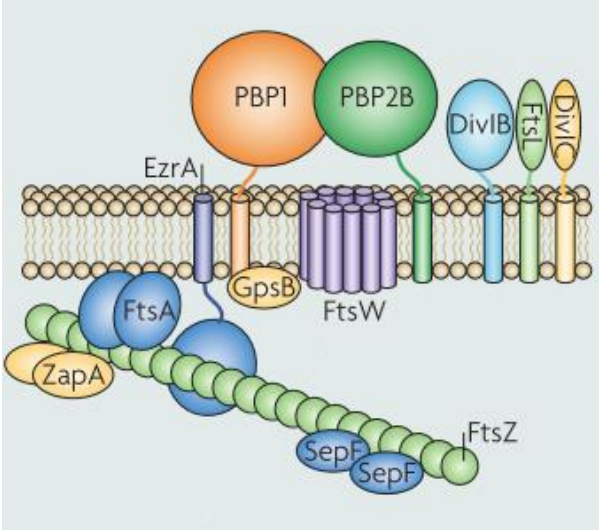

Figure 1.1 Divisome assembly in *B. subtilis.* The formation of the divisome starts with the recruitment of the early divisome proteins (FtsA, EzrA, ZapA and SepF) to the Z-ring by FtsZ. Later, the later divisome proteins (DivIB, DivIC, FtsW, FtsL, PBP2B, GspB, PBP1) are assembled onto the Z-ring in a concerted and interdependent manner, as opposed to the linear mode of recruitment of these proteins in *E. coli* (Adams and Errington, 2009).

1.2.2 Cell Wall Synthesis

Cell wall is a sturdy structure, which enables building and maintenance of cell shape and withstands cell's intracellular pressure (Graumman, 2012b). The cell wall stiffness of both gram-positive and gram-negative bacteria is provided by peptidoglycan. PG or murein is a hetero-polymer built up of linear glycan chains cross-linked through peptide bridges. The glycan chains are made of alternating subunits of β-1,4-linked N-

acetyl-glucosamine (GlcNAc) and N-acetyl-muramic acid (MurNAc) subunits **(Fig.1.2).** The glycan chains have few variations between different bacterial species, but there is considerable variation in the composition of stem peptides that are linked to the carboxyl group of MurNac (Schleifer and Kandler, 1972; Scheffers and Pinho, 2005). The length of glycan chains is also different between bacterial species, since in *S. aureus* PG strands are shorter than in *E. coli* and *B. subtilis*. The length of the peptide chains can also differ (tri-, tetra-, pentapeptide) (Vollmer and Bertsche, 2008). Despite of its stiffness, PG is an elastic structure, which can reversible expand and shrink without breaking (Koch and Woeste, 1992). The cell wall stability implies a fine control of the insertion and removal of wall material by enzymes capable of synthesizing or hydrolyzing the PG layers.

In all of these bacteria stem peptides are pentapepide chains, which only differ in the dibasic amino acid composition. Whereas mesodiamoinopimelic acid (*m*-A_2pm) is present in *E. coli* and *B. subtilis*, L-Lysine (L-Lys) is the dibasic amino acid in *S.aureus*. Therefore, the composition of a newly synthetized stem peptide is L-Ala–D-Glu–*m*-A_2pm/L-Lys–D-Ala–D-Ala, containing L-Ala bounded to the MurNac. Additionally in *S.aureus*, L-lys is attached to a pentapeptide of Glycines (Gly), forming a flexible pentaglycine cross bridge, which is responsible for the high degree of cross-linking observed in these bacteria. PG is formed via two basic processes: assembly of glycan chains (transglycosylation) and peptide cross bridge formation (transpeptidation) (Scheffers and Pinho, 2005). Unlike gram-positives *B. subtilis* and *S. aureus*, *E. coli* has an outer membrane, containing lipoprotein (Braun's lipoprotein, LPP) attached to PG that contributes to stability of the cell envelope in gram-negative bacteria (Scheffers and Pinho, 2005; Vollmer and Bertsche, 2008). On the other hand, *B. subtilis* and *S. aureus* thick cell wall is enriched with charged polymers, teichoic and teichuronic acids, and proteins anchored to the cell wall. To date two models have been proposed for the PG orientation, which consider either a parallel or a perpendicular arrangement of the glycan strands towards to the cytoplasmic membrane (Vollmer *et al*., 2004; Dmitriev *et al*., 2003).

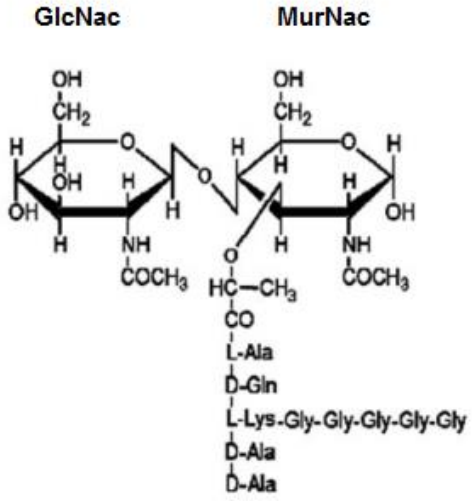

Figure 1.2 Primary structure of *S. aureus* peptidoglycan. The overall bacterial peptidoglycan is composed of linear glycan chains linked through pentapeptide cross-bridges. N-acetyl-glucosamine (GlcNAc) and N-acetyl-muramic acid (MurNAc) disaccharide subunits are bound together by a β-1,4 linkage. Each pentapeptide, known as stem peptide, is composed of L-Ala–D-Glu–DA–D-Ala–D-Ala. The carboxyl group of MurNAc is linked to the L-Ala of a stem peptide. The dibasic amino acid (DA) present in *S. aureus* is L-Lys, which is attached to a pentaglycine bridge and confers a high level of PG cross-linkage. Adapted from Scheffers and Pinho, 2005.

PG biosynthesis occurs in three sequential stages: i) Synthesis of the PG precursor by specific enzymes and linkage to the carrier lipid (undecaprenyl-phosphate or bactoprenol), ii) Flipping across the membrane, iii) Incorporation of the precursor into the cell wall (Vollmer & Bertsche, 2008).

In the first stage, the intermediates of PG precursor synthesis Uridine diphosphate-N-acteyl-glucosamine (UDP-GlcNAc) and uridine diphosphate-N-acteyl-muramic acid (UDP-MurNAc), are formed in the cytoplasm (**Fig.1.3**). UDP-MurNac is originated from UDP-GlcNac. L-Ala, D-Glu, *m*-A_2pm and a D-Ala–D-Ala dipeptide are successively added to the peptide side chain (linked to UDP-MurNAc) by ATP-dependent ligases MurC, MurD, MurE and MurF, respectively. The D-amino acids are generated from L-amino acids by racemases. Before transport of hydrophilic precursors across the cytoplasmic membrane, a lipid carrier (bactoprenol) is attached by MraY to form lipid I (undecaprenyl pyrophosphoryl-MurNAc-pentapeptide). Then, GlcNAc is added to lipid I by MurG, yielding lipid II (undecaprenyl pyrophosphoryl-GlcNAc-β-(1, 4)-MurNAc-pentapeptide). The coupling of a disaccharide precursor (hydrophilic substrate) to a lipid molecule facilitates its translocation through the hydrophobic membrane (van Heijenoort, 2001; Vollmer and Bertsche, 2008).

During the second stage, Lipid II is transported across the cytoplasmic membrane to the periplasmic site at the outer membrane by a flippase or specific translocase (Vollmer and Bertsche, 2008). It is though that the integral membrane homologues, FtsW and RodA (or mrdB) function as translocases of lipid precursors across the cytoplasmic membrane, which may then be directed to their cognate PBPs (Scheffers and Pinho, 2005). In *E. coli* lipid II is translocated to the periplasmic site by FtsW, localized at the septum. It is likely that *S. aureus* lipid II is translocated by an homologue of FtsW (Pinho *et al*., 2013).

In the third stage, lipid II precursors are incorporated into the cell wall, to cause enlargement of the synthetized peptidoglycan. This reaction is catalyzed by murein synthases, transpeptidases (TPases) and tranglycosylases (TGases), which have transmembrane and cytoplasmic domains and perform their actions through their transglycosylation and transpeptidation periplasmic domains. Transglycosylation is responsible for formation of the glycan strands from lipid II substrate (van Heijenoort, 2001). Transpeptidation enables cross-linking between the peptides and takes place when a TPase links D-ala from one stem peptide to the m-A_2pm (*E. coli* and *B. subtilis*) or the pentapeptide glycine bridge (*S.aureus*) of

the next stem peptide (van Heijenoort, 2001; Scheffers and Pinho, 2005). PG is concomitantly formed and degraded by specific enzymes, named PG synthases and murein hydrolases. PG synthases with a TPase activity are termed Penicillin-binding proteins (PBPs), due to their capacity of binding Penicillin and other β-lactams, which are structurally similar to the D-Ala-D-Ala termini of the stem peptides (Vollmer and Bertsche, 2008).

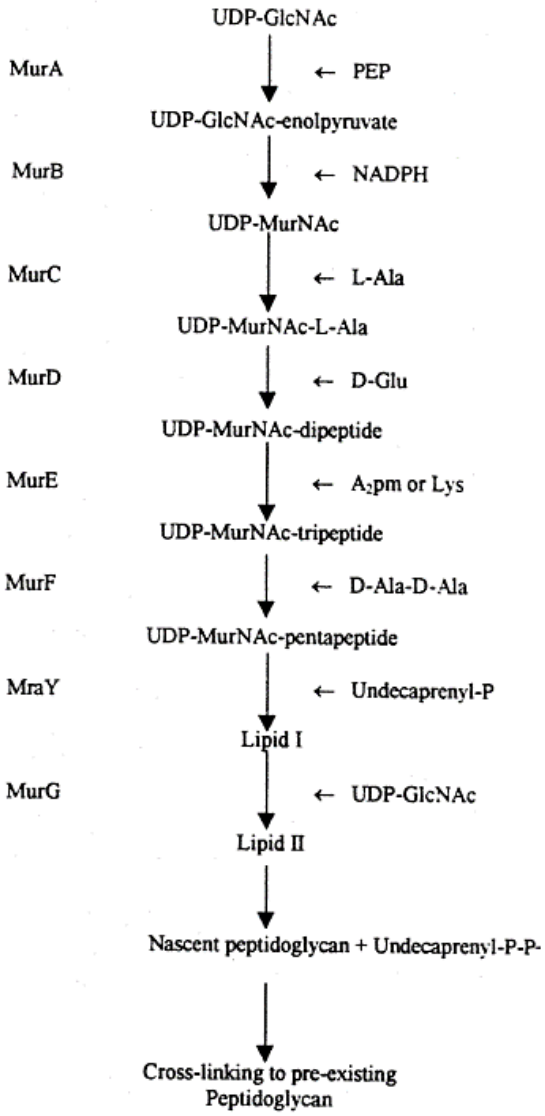

Figure 1.3 Peptidoglycan biosynthesis. In the first stage, the intermediates of PG precursor synthesis UDP-GlcNac and UDP-MurNac are assembled in the cytoplasm via addition of UDP precursors and lipid intermediates. The cytoplasmic enzymes MurA to MurF catalyze the formation of the UDP-MurNAc-pentapeptide precursor from UDP-GlcNAc. MraY catalyzes the transfer of the phospho-MurNAc- pentapeptide moiety of UDP-MurNAc-pentapeptide to the membrane acceptor, undecaprenyl phosphate, yielding lipid I. Then, GlcNAc is added to lipid I by MurG, yelding lipid II, which carries the PG precursor GlcNAc-MurNAc- L-Ala-γ-D-Glu-A2pm(or L-Lys)-D-Ala-D-Ala. During the

second stage, lipid II precursor is transported through the hydrophobic membrane to the periplasmic site by a flippase or specific translocase, where it is incorporated into nascent peptidoglycan. In the third stage, lipid II precursors are incorporated into the pre-existing cell wall, by murein synthases or PG synthases, known as PBPs, which have transpeptidation and transglycosylation activities. Adapted from van Heijenoort, 2001.

B. subtilis and *E. coli* are proposed to have two modes of cell wall synthesis, i) through elongation of the lateral wall and ii) through formation of a division septum (Scheffers and Pinho, 2005). More recently, another model for cell wall synthesis, which divides the first mode (elongation) into two, dispersed elongation and pre-septal elongation, was proposed. Dispersed elongation occurs firstly with the insertion of PG in several sites of the lateral wall; the tubulin homologue FtsZ locates then to the mid-cell to drive "preseptal" elongation (Typas *et al*., 2012). *S. aureus* cell wall synthesis is discussed below.

1.3 Penicillin-binding proteins (PBPs)

PBPs are classified as acyl serine transferases and are divided into high-molecular-weight (HMW) PBPs, low-molecular-weight (LMW) PBPs, and β-lactamases. HMW PBPs contain two domains, a C-terminal domain, located in the periplasm and a short N-terminal transmembrane domain that anchors the protein to the membrane. They are grouped into Class A and Class B PBPs, bifunctional or monofunctional enzymes, depending on the composition of the N-terminal domain. In Class A PBPs, the C-terminal domain is a penicillin-binding domain (PB module) with TP activity (responsible for cross-linking between peptides) linked to an N-terminal domain that contains TG activity (participates in glycan strands polymerization). Class B PBPs contain a C-terminal PB module with TP activity and an N-terminal non-penicillin binding (n-PB) module with presumable functions as a chaperone, in cell morphogenesis, or in control of cell division (Ghuysen, 1991; Scheffers and Pinho, 2005). LMW PBPs are monofunctional DD-peptidases, mostly DD-carboxypeptidases that catalyze the hydrolysis of the carboxyl terminal D-ala–D-ala of a stem peptide. Although, some, have TPase (such as *S. aureus* PBP4) or endopeptidase activities (Scheffers & Pinho, 2005). Besides PBPs, another class of proteins, called monofunctional transglycosylases (MGTs), contains TG activity.

The analysis of mutants containing mutations in several PBPs and the localization of PBPs by fluorescence microscopy has provided new information about the function of these enzymes and the identification of the place where PG synthesis occurs.

The model organisms *E. coli* and *B. subtilis* have 12 and 16 PBPs, respectively with specific functions in PG synthesis during different stages of cell growth (Scheffers and Pinho, 2005). However, the

fact that most of these PG synthesizing enzymes have redundant functions makes the study of their functions a difficult task (Scheffers and Pinho, 2005; Pinho and Errington, 2005).

1.3.1 *S. aureus* PBPs

S. aureus seems to be a better candidate to study the role and possible interactions between PBPs, as it has only 4 to 5 PBPs. Four native PBPs, PBP1, PBP2, PBP3 and PBP4 are present in MSSA strains and an extra PBP2A is only present in MRSA strains and is responsible for β-lactam resistance, due to its low affinity to these antibiotics (Scheffers and Pinho 2005; Hartman and Tomasz, 1984). PBP2 is a class A PBP, containing both TPase and TGase activities (Goffin and Ghuysen, 1998; Murakami *et al*., 1994).

In the presence of oxacillin, PBP2 TPase domain becomes acylated and thus is unable to bind to its pentapeptide substrate. Moreover, PBP2 loses its ability to localize to the division septum and perform its role in cell wall synthesis. Under these conditions, cells exhibit a dispersed mode of cell wall synthesis in confined spots at the periphery of the cell (Pinho and Errington, 2005). Unlike methicillin sensitive *S.aureus* strains, MRSA strains contain an extra PBP, PBP2A that is able to replace PBP2 function as a TPase in presence of β-lactams (Pinho *et al*., 2001b). However, PBP2 is still required for cell survival as its TGase domain seems to cooperate with the TPase domain of PBP2A (Pinho *et al*., 2001). Moreover, in these strains PBP2 is not delocalized from the septum suggesting that PBP2A maintains acylated PBP2 at that place (Pinho and Errington, 2005).

PBP1 is a class B HMW monofunctional TPase essential for cell growth and survival in MRSA and MSSA strains. In the absence of PBP1, cells are unable to divide and lose their viability (Okonog *et al*., 1995; Wada and Watanabe, 1998; Pereira *et al*., 2007). PBP1 localizes mainly to the division septum (Pereira *et al*., 2007). Loss of the functional TPase domain of PBP1 resulted in minor alterations in PG composition, and in a process that may repress the expression of autolytic genes and thus, prevent cell separation (Pereira *et al*., 2009). Therefore, it is suggested that the essential activity of PBP1 as a TPase is related to the control of cell division instead of having a direct role in PG cross-linking (Pereira *et al*., 2007; Pereira *et al*., 2009).

PBP4 is a LMW non-essential TPase involved in secondary cross-linking of PG (Wyke *et al*., 1981). As it is required for synthesis of highly branched peptidoglycan, depletion of PBP4 leads to a decrease in PG cross-linking (Wyke *et al*., 1981; Sieradzki *et al*., 1999; Memmi *et al*., 2008). Moreover, together with PBP2A, PBP4 contributes to β-lactam resistance in CA-MRSA (but not HA-MRSA strains), since loss of PBP4 causes an increase in susceptibility to these antibiotics (Memmi *et al*., 2008). It has been proposed that PBP4 is recruited to the division septum by an intermediate of wall teichoic acid (WTA) synthesis localized at that place, based on the following observations; i) In the absence of wall teichoic acids synthesis,

PBP4 is delocalized (becomes dispersed over the cell membrane) and is not functional; ii) Synthesis of WTA was shown to be required for PBP4 recruitment to the division septum (Atilano *et al*., 2010).

PBP3 is a non-essential monofunctional TPase which localization remains unknown (Pinho *et al.*, 2000; Scheffers and Pinho, 2005).

1.4 Evidence for multienzyme complexes formed by PBPs

Many studies have provided support for the existence of multienzyme complexes formed by PBPs in several bacteria (Bhardwaj and Day, 1997; Alaedini and Day, 1999; Figge *et al*., 2004; Simon and Day, 2000). Based on previous reported interactions between murein synthases and hydrolases in *E.coli,* it has been proposed that this organism forms two multienzyme complexes, which play a role in cell wall synthesis either during cell elongation or cell constriction, called murein-synthetizing machinery. They are similar but have different specificities based on the presence of PBP2 (elongation complex) or PBP3 TPases (constriction complex). This model of PG assembly has been identified in other gram-negative bacteria, being in agreement with the "three-for-one" model that states that insertion of three new glycan strands in the cell wall is concomitant with removal of one strand (**Fig.1.4**) (Höltje, 1996; Höltje, 1998; Scheffers and Pinho, 2005).

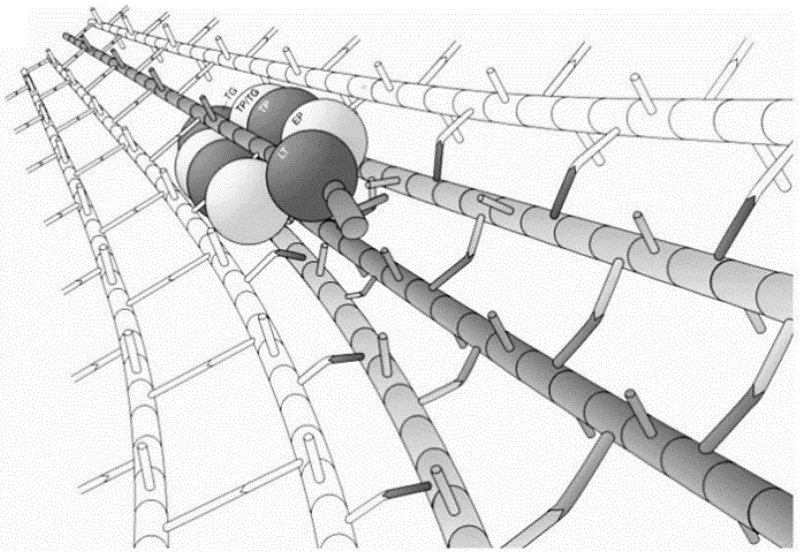

Figure 1.4 Hypothetical murein-synthetizing machinery formed by gram-negative bacteria. It is proposed that a multiprotein complex is responsible for i) synthesizing three new cross-linked glycan strands (shown in gray). A bifunctional PBP, PBP1A or PBP1B, with TPase and TGase (TP/TG) activities dimerizes and joins a pre-existing PG strand to form a murein triplet, which is connected to the strand by transpeptidation, catalyzed by a dimer of either PBP2 or PBP3 TPases (TP); ii) Simultaneously attaching the newly synthesized strands to a docking strand in both

sides of the peptide bridges (middle gray strand) and degrading the docking strand by action of hydrolases. A dimeric endopeptidase (EP; PBP4 or PBP7) splits the peptide cross-bridges of the old strand while a lytic TGase (LT; Slt70, MltA, or MltB) depolymerizes the glycan strand. Strands shown in white represent preexisting strands (Höltje, 1998).

In *B. subtilis*, isolation of PBPs by chromatography has revealed that these enzymes form two multi-protein complexes, composed of either three or seven PBPs (Simon and Day, 2000).

Importantly, in *S. aureus,* EzrA was found to interact with several divisome proteins, including PBP1, PBP2 and PBP3, suggesting that these proteins form a complex that plays a role in cell division (Steele *et al.*, 2011). More recently, it was reported that an *S.aureus* minimal strain (lacking non-essential genes for peptidoglycan synthesis) that contains only 7 of 9 seven PG synthesizing-enzymes, is able to normally grow and divide. Therefore, it was shown that *S. aureus* can use a minimal PG synthesis machine, composed of a TPase (PBP1) and a bifunctional PBP (PBP2) to catalyze PG synthesis (Reed *et al*., 2015). Therefore, more data is needed to prove the existence of a multi-enzymatic PG synthesis complex in gram-positive bacteria.

1.5 Divisome and cell wall synthesis machinery of *S.aureus*

S. aureus contains homologues for all the essential genes for cell division in *B. subtilis* (Steele *et al., 2011)*. Furthermore, as PG synthesis seems to take place mainly at one division site (septum), according to Pinho and colleagues, there should only be one PG synthesizing complex of *S. aureus*, located at the division site (Steele *et al*., 2011; Pinho *et al*., 2013).

PBP1, PBP2 and PBP4 localize to the division septum, site where PG synthesis occurs. These PG synthetizing enzymes are recruited to the division septum by different mechanisms (Pinho *et al*., 2013). PBP1 is suggested to be a component of the divisome and seems to be recruited by an unknown divisome protein in a manner independent of its activity as a TPase (Pereira *et al*., 2007; Pereira *et al*., 2009). PBP2 localizes to division septum may be dependent on recognition by its substrate. In the beginning of septum formation PBP2 localizes in a ring and, as the septum closes, it localizes all over the septum (Pinho and Errington, 2005). PBP4 is recruited to the septum by an intermediate of WTA synthesis (Atilano *et al*., 2010).

The proposed model for cell wall synthesis in *S. aureus* requires the recruitment in the first place of two essential proteins, PBP1 and PBP2, to the division septum (**Fig.1.5**). Then, WTA are synthetized at the division septum, where they are attached to PG. PBP4 is later recruited to the septum and increases PG cross-linking through its transpeptidation activity. The splitting of the septum requires the remodeling and

hydrolysis of the septal PG by autolysins (cell wall hydrolases). The full septum is composed of a low-density central region, which does not extend into the surface cell wall, separated by two high-density regions, which will each constitute half of the new cell wall in daughter cells after splitting. This suggests that autolysins only act at the periphery of the septum (Pinho *et al*., 2013). This model considers that the newly formed cells remain spherical over the cell cycle.

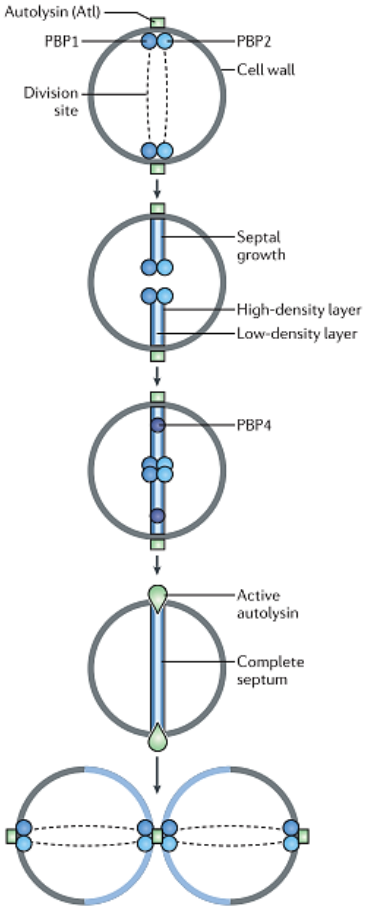

Figure 1.5 First model of cell wall synthesis in *S. aureus*. This model considers that peptidoglycan is synthesized only at the septum, in a process that initiates with the recruitment of PBP1 and PBP2 to that place. At a later stage, PBP4 is recruited to the septum, where it contributes to increasing peptidoglycan PG cross-linking. The full septum is composed of a low-density central layer separating two high-density layers, corresponding to adjacent cross walls, which will each constitute half of the new cell wall in daughter cells after splitting. In *S.aureus*, a specific autolysin is responsible for the septum splitting, acting at the periphery of the septum (Pinho *et al*., 2013).

However, the model of cell wall synthesis was recently redefined. It was discovered that the proportion of new cell wall material versus old cell wall in the newly formed cells is not 50%-50% but instead ~ 33%-

67%, respectively. This suggests that there is a second mode of cell wall synthesis in *S. aureus* through enlargement of the lateral wall (Monteiro *et al*., 2015) (**Fig.1.6**).

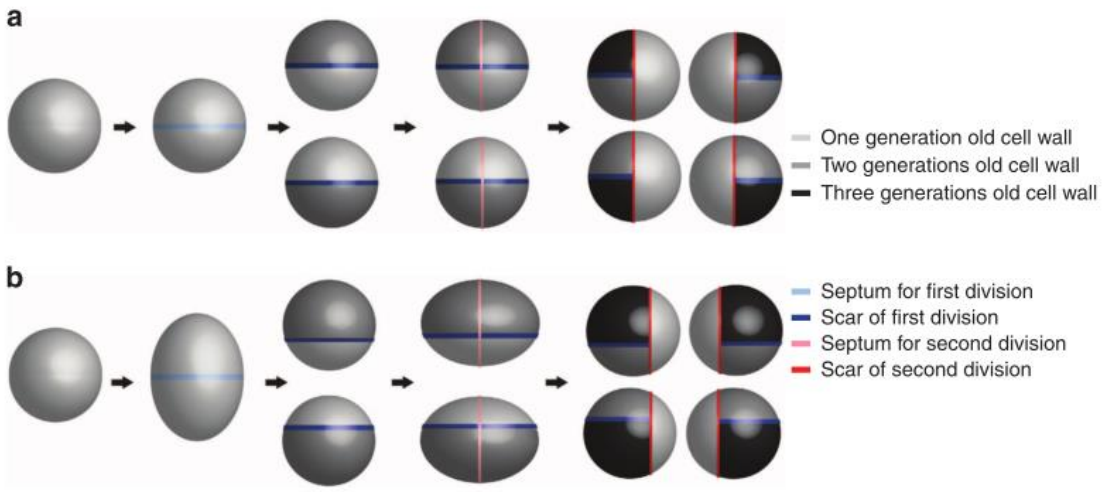

Figure 1.6 Two models of cell wall synthesis in *S. aureus*. The previous model (a) proposes that cell wall material of half of each newly formed cell is made from the septum of the mother cell. Therefore the daughter cells have a proportion of 50% of old cell wall material and 50% of new cell wall material, and the spherical shape is maintained throughout the cell cycle. The new model (b) assumes that in the beginning of the cell cycle cells are spherical and elongate over the cell cycle. The cell wall material deposited from the septum of the mother cell (new cell wall) constitutes only ~33% of the surface area of each daughter cell, while the cell wall material resulting from one hemisphere of the mother cells (old cell wall) occupies ~67% of the daughter cell (Monteiro *et al*., 2015).

1.6 Evidence for cooperative interaction between FtsZ and EzrA

In *B. subtilis*, EzrA was found to be localized to the cell membrane where it acts as a negative regulator of FtsZ, as it inhibits Z-ring formation outside the mid-cell (at medial and polar sites), therefore preventing aberrant cell division (Levin *et al*., 1999). Moreover, EzrA co-localizes with FtsZ to the nascent septal site, suggesting a positive role for EzrA in cell division, by maintaining Z-ring assembly and dynamics (Levin *et al*., 1999; Haeusser *et al*., 2004). This observation suggests that EzrA may be responsible for coordinating cell growth and cell division (Haeusser *et al*., 2007). Accordingly, EzrA was shown to recruit PBP1 to the divisome, promoting cell separation and subsequent elongation associated-cell wall synthesis. Therefore, in rod-shaped bacteria, EzrA coordinates the two modes of cell wall synthesis (through cell division or cell elongation) (Claessen *et al*., 2008).

In coccoid *S. aureus*, EzrA interacts with FtsZ at the mid-cell, the main place where PG synthesis takes place, and furthermore it is required for proper assembly of the divisome at the mid-cell (Pinho and

Errington, 2003; Steele *et al*., 2011). The simultaneous interaction of EzrA with FtsZ, other divisome components and PBPs has led to the hypothesis that this protein acts in the linkage between cytoplasmic FtsZ and the PG synthetizing machinery located in the periplasm (Steele *et al*., 2011; Jorge *et al*., 2011).

1.7 Evidence for cooperative functioning of PBP2 and PBP4 in *S.aureus*

As described above, the TGase activity of PBP2 and the TPase activity of PBP2A are required for cell survival in MRSA strains, upon challenging with β-lactams. Importantly, when PBP2 TGase domain was affected by a point mutation, the length of PG glycan strands was reduced (Pinho, *et al*., 2001). Moreover, a single PBP2 point mutation in the TPase domain was shown to cause a decreased affinity for a β-lactam (ceftizoxime) with high selective affinity for PBP2. This drug-resistance phenotype was accompanied by a reduced proportion of highly cross-linked PG and increased proportion of monomeric and dimeric muropeptide monomers and dimers. This discovery suggested not only a role for the TPase domain of PBP2 but also a link between PBP2 and PBP4 in secondary cross-linking (Leski and Tomasz, 2005). Likewise, in CA-MRSA, when cells are challenged with oxacillin and depleted from PBP4, the transcription of PBP2 is altered, thus causing a decrease in secondary PG cross-linking (Memmi *et al*., 2008). This finding supports the hypothesis of a concerted action between these two proteins in cell wall cross-linking (**Fig.1.7**).

PBP2 and PBP4 contribute not only to resistance against β-lactams but also to resistance to the one of the last resort antibiotics effective against *S. aureus,* vancomycin**.** Decreased levels of PG cross-linking are a common feature in VRSA strains due to PBP4 inactivation. It is suggested that the alteration of cell wall composition is a mechanism by which these strains survive in presence of vancomycin (Sieradzki and Tomasz, 1997; Sieradzki *et al*., 1999). Accordingly, PBP2 mutants are more susceptible to vancomycin, suggesting that PBP2 may play a major role in the cell wall assembly of VRSA strains (Sieradzki and Tomasz,1999).

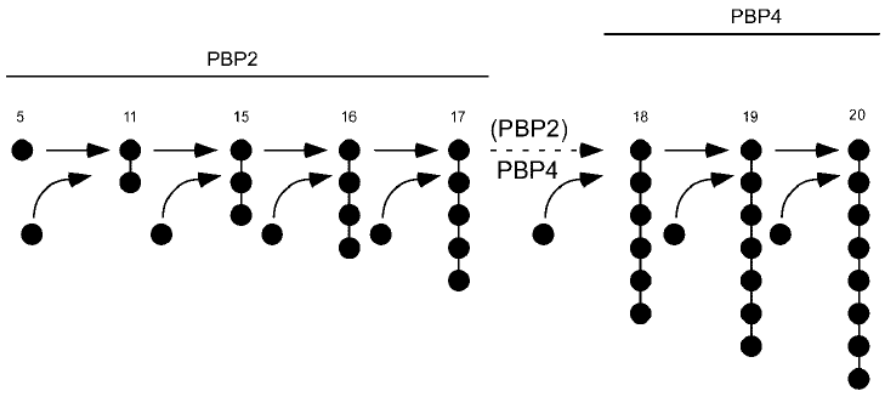

Figure 1.7 Model for cooperative functioning of PBP2 and PBP4. This model suggests that the TPase activity of PBP2 may produce muropeptide dimers (peptide 11), trimers (peptide 15), tetramers (peptide 16) and pentamers (peptide

17), which would be used as a substrate for PBP4 activity. PBP4 would therefore add the donor monomeric peptides to the more highly cross-linked acceptor peptides (peptides 18,19, 20), in order to form a highly cross-linked cell wall. Accordingly, in a double mutant of PBP2 and PBP4, there is accumulation of monomeric muropeptides, which prevents cross-linking of between wall components to form a highly cross-linked PG (Leski and Tomasz, 2005).

1.8 Methods for detection of protein-protein interactions

To study protein complexes it is crucial to determine which proteins interact to each other. Most approaches used for screening of interactions between two or more proteins involve assays performed *in vitro*, such as pull down assay and co-immunoprecipitation (Kodama and Hu, 2012). However, these approaches do not exclude potential artifacts that can result from cell manipulation and most of them require purification of proteins from their native environments (Kerppola, 2006; Kerppola, 2008). Moreover, these methods do not reveal the cellular place(s) where protein complexes are formed and, more importantly, do not address interactions that only exist in a specific phase of the cellular cycle. An alternative to these methods is *in vivo* bacterial two-hybrid (BTH) assay, which enabless identification of the interactions between putative components of the divisome, but it does not determines where (sub-cellular place) and when (cell cycle phase) these proteins interact (Steele *et al.*, 2011).

1.8.1 BiFC: A fluorescence protein complementation assay

Fluorescent proteins (FPs) have started to be used for visualization of protein interactions in complementation assays. Among these FPs are green fluorescent protein (GFP) and yellow fluorescent protein (YFP) (Kerppola, 2008).

Bimolecular fluorescence complementation (BiFC) assay is a powerful tool that, unlike methods described above, enables direct visualization of protein-protein interactions in living cells. This assay is based on complementation of two non-fluorescent fragments of a FP when they are brought together by interactions between proteins fused to each fragment (Kerppola, 2008; Hu *et al*., 2002). Furthermore, it has many other advantages over previous described methods, including: examination of protein interactions occurs in their normal cellular environment; determination of subcellular localization of protein interactions; high intrinsic fluorescence formed by the protein complex and minimization of alterations caused by experimental manipulation. Nevertheless, this method reveals a delay between the time when the complex is formed (i.e. when the interaction occurs) and the time when the complex becomes fluorescent, which is mostly related to the slow rate of folding of the fluorescent proteins (Kerppola, 2006; Kerppola, 2008).

Despite not detecting real-time interactions it enables detection of transient and weak interactions, as interaction between the proteins can stabilize FP association (Kerppola, 2008).

1.8.2 Applications of BiFC

BiFC was firstly developed to examine proteins interactions among bZip family transcription factors in *E.coli*. YFP was divided into two fragments, YC and YN, at non conserved amino acid residues within loops at either end of the β-barrel structure, and these fragments were fused to the C-terminal ends of Basic Leucine Zipper Domain (bZIP domain) of Fos and Jun. Fos and Jun are transcription factors containing a bZIP domain which was shown to dimerize (Gentz *et al*., 1989). The authors have firstly validated this system *in vitro*, having demonstrated that fragments of YFP can reconstitute the fluorophore when fused to proteins that interact with each other. They have also proven that formation of the BiFC complex depends on the native interface of fusion proteins. Importantly, they have shown that fluorescence complementation between bFosYC and bJunYN is not a result from interactions between YFP fragments. As a result, the bFosYC-bJunYN complex was localized in mammalian cells by fluorescence microscopy (Hu *et al*., 2002). Likewise, similar studies have successfully detected pairwise interactions between gram-negative *E. coli* early divisome components (among FtsZ, FtsA and ZipA, ZapA and ZapB) or gram-positive *B. subtilis* actin-like proteins (among MreB, MreBH and Mbl), responsible for cell morphology and chromosome segregation (Soufo and Graumann, 2006; Pazos *et al*., 2013).

Importantly, in all of these approaches, an enhanced version of YFP (eYFP) was split between amino acid residues 154 and 155, producing an N-terminal fragment (YFPN) composed of residues 1–154 and a C-terminal fragment (YFPC) made of residues 155–238. **Figure 1.8** illustrates the principle of BiFC.

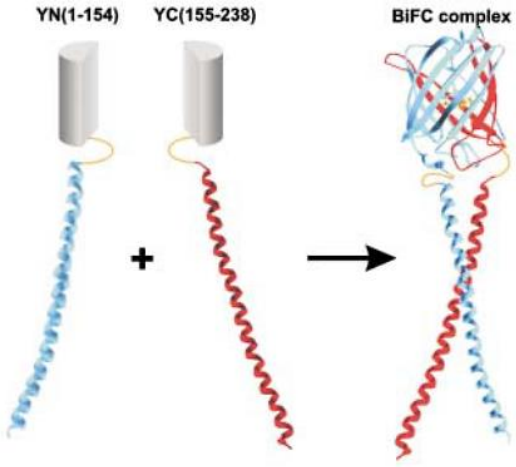

Figure 1.8 Principle of Bimolecular fluorescence complementation assay (BiFC). YFP is split between amino acid residues 154 and 155, resulting in an N-terminal (YN) and a C-terminal (YC) fragment. Two putative interacting proteins are covalently linked to either one of both YFP fragments. If these proteins interact, association of YFP fragments occurs and mediates reconstitution of the fluorophore, which enables formation of a bimolecular fluorescent complex. Adapted from Hu *et al*., 2002.

1.8.3 GFP scaffold and possible split-sites

Aequorea GFP variants have been mutagenized in the past several years in order to produce brighter and more photostable derivatives. All the resulting FPs share the same structure, in which a large polypeptide is wrapped into 11 β-sheets that surround a central α-helix containing the fluorophore, with short helical segments in both ends of the polypeptide (Shaner, Patterson, & Davidson, 2007). Circular permutation is a method that enables alteration of the amino acid order in a protein sequence (Yu and Lutz, 2011). Several studies used this method to determine the places in GFP where an insertion can be introduced without affecting its overall structure and protein folding. Likewise, it was determined that GFP can be split at positions in the loop between the 6th and 7th β-strands, in the 7^{th} β-strand, in the loop between the 7th and 8th β-strands, in the 8th β-strand, and in the loop between the 8th and 9th β-strands (Kodama and Hu, 2012). These positions were later employed by Hu and its colleagues to split YFP for development of the BiFC assay.

1.9 Aim of the thesis

PBPs represent the target of many antibiotics important for treatment of MRSA infections, such as β-lactams. Moreover, PBPs are essential for cell wall integrity, as they are involved in the last stages of PG synthesis. Without proper PG synthesis the integrity of the cell wall is disrupted and cell survival is compromised (Vollmer and Bertsche, 2008). PBPs have been found to be part of a multi-protein complex that acts in a concerted manner in building the cell wall synthesis without compromising cell integrity (Höltje, 1996; Höltje, 1998; Scheffers and Pinho, 2005). Importantly, it has been shown that *S. aureus* uses a minimal PG synthesizing machinery, composed of two essential PBPs (PBP1 and PBP2), essential for cell survival. However, non-essential PBPs, such as PBP4, are also important in more challenging environments, as they are involved in antibiotic resistance of *S. aureus* (Reed *et al*., 2015). PBP2 and PBP4 have been related with resistance to earlier effective antibiotics, such as β-lactam methicillin and glycopeptide vancomycin (Sieradzki *et al*. 1999; Pinho *et al*., 2001a; Pinho and Errington, 2005). They have been proposed to play a cooperative functioning in cell wall synthesis of *S. aureus* resistant strains (Leski and Tomasz, 2005). However, factual information about their interaction in living cells is lacking.

Early studies to detect protein interactions among cell division or cell wall synthesis components have focused mainly in methods *in vitro* (Kodama and Hu, 2012). Unlike these, BiFC allows to visualize transient protein interactions *in vivo*. This system has successfully identified divisome interacting partners in *E. coli* and interactions between cell shape and chromosome segregation proteins in *B. subtilis*, but has not yet been employed in *S. aureus* (Soufo and Graumann, 2006; Pazos *et al*., 2013).

The aim of this thesis is to determine if PBP2 and PBP4 interact during *S. aureus* cell cycle by using a BiFC system. For that purpose we developed a split-GFP_{P7} system, an approach that follows the same principle as BiFC, except that an improved version of GFP, GFP_{P7} (Fisher and DeLisa, 2008) is used. The discovery of a physical interaction between PBP2 and PBP4 and the determination of the subcellular sites where these proteins interact would give more clues about their role in cell wall synthesis and later on could aid in the identification of new antimicrobial targets against this pathogen.

2. MATERIAL AND METHODS

2.1 Bacterial strains, plasmids and growth conditions

The *E. coli* strain DC10B was used for cloning and plasmid propagation. Strains were stored at -80°C by adding 300 µl 50% (v/v) glycerol to 700 µl overnight culture. *E. coli* strains were grown at 37ºC or 30°C on Luria-Bertani agar (LA) or with aeration in Luria–Bertani broth (LB, Difco), supplemented with ampicillin (100 µg/ml) as required. *S. aureus* strains were grown at 37ºC or 30°C with aeration on Tryptic soy agar (TSA, Difco) or in Tryptic soy broth (TSB, Difco). When necessary, the medium was supplemented with the following antibiotics and inducers: erythromycin (Erm) 10 µg/ml; kanamycin (Kan) 50µg/ml; neomycin (Neo) 50 µg/ml; chloramphenicol (Cm) 10 µg/ml; (Sigma-Aldrich); isopropyl-b-D-thiogalactopyranoside (IPTG, Apollo Scientific) 0.5 mM; 5-bromo-4-chloro-3-indolyl-b-D-galactopyranoside (X-Gal, VWR) 100 µg/ml; Cadmium Chloride anhydrous ($CdCl_2$, Fluka) 0.1 µM and 0.05% xylose (Xyl, Sigma-Aldrich). Growth was monitored by the increase in optical density at 600 nm (OD_{600} nm), measured using a spectrophotometer (Ultrospec 2100 pro Amersham Biosciences).

2.2 Molecular biology

2.2.1 Purification of plasmid DNA from *E. coli*

Plasmid DNA was purified from *E. coli* DC10B cells using Wizard Plus SV Miniprep DNA Purification System protocol (Promega), following the manufacturer's instructions. When higher amounts

were needed, after plasmid extraction, DNA was precipitated by adding 1:10 volume of Sodium acetate (3M, pH 5.2, Sigma-Aldrich) and 3.0x volume of 95% ethanol. After incubation on ice for 15 min, plasmid DNA was centrifuged at 14,000 rpm for 30 min at 4°C. DNA pellet was rinsed with 70% ethanol, centrifuged again for 15 min and dissolved in miliQ water. Plasmid DNA was stored at 4°C.

2.2.2 Isolation of genomic DNA from *S.aureus*

Genomic DNA was extracted from *S. aureus* COL cells grown overnight in TSB, at 37°C. Cells were harvested from 500 μl cultures and resuspended in 100 μl EDTA 50mM (Sigma-Aldrich). 1 μl lysostaphin 10 μg/mL (Sigma) and 2 μl RNase 20 μg/mL (Sigma) were added and following incubation for 30 min at 37°C, cells were incubated at 80°C with Nuclei Lysis solution (Promega) for 5 min. After cooling at room temperature, 200 μl Protein Precipitation Solution (Promega) was added to the cell suspension, which was then incubated on ice for 10 min. Cell suspension was centrifuged at 13,000 rpm for 20 min and DNA was precipitated with isopropanol. After being centrifuged again for 10 min, DNA pellet was washed with 70% ethanol, centrifuged for 3 min and ethanol the pellet was allowed to air-dry. Finally, DNA pellet was resuspended in 200 μl sterile miliQ water.

2.2.3 Polymerase Chain reaction (PCR)

The sequences of primers, purchased from Metabion, used in this study are listed in **Table 2.1**. PCR reactions derived from molecular cloning were performed with Phusion polymerase (Thermo Scientific) and with GoTaq polymerase (Promega) or DreamTaq Polymerase (Thermo Scientific) for colony screenings, according to manufacturer's instructions. Details of reaction programs are shown below.

Reaction programs

Molecular cloning	Colony screenings
98° Pre-Denaturation: 1 min	98° Pre-Denaturation: 7 min
98°C Denaturation: 10 sec	98°C Denaturation: 10 sec
56°C Annealing: 30 sec	56°C Annealing: 30 sec
72°C Extension: 30 sec per 1 kb	72°C Extension: 1 min per 1 kb
Repeat 30 cycles	Repeat 30 cycles
72°C Final extension: 7 min	72°C Final extension: 7 min
4°C Pause	4°C Pause

2.2.4 Sequencing

Sequencing reactions were carried out at GATC Biotech using Sanger Sequencing. Reactions were prepared by adding 5 µl of plasmid miniprep (80-100 ng/ml) or PCR product (20-80 ng/ml) to 1.25µl primer (20mM) and ddH_20 (up to 10 µl). The resulting sequences were compared to a predicted/database sequence using SeqMan from DNASTAR Lasergene 11 software.

2.2.5 Restriction digestion and ligation of DNA

Before restriction digestion, PCR fragments were purified using PCR-clean up System protocol (Promega), following the manufacturer's instructions. Plasmid DNA and PCR fragments were digested with FastDigest restriction enzymes (Thermo Scientific). For cloning, PCR fragments were digested in a 40 µl reaction using 20 µl PCR product, 4µl 10X FastDigest Buffer, 1µl restriction enzyme and miliQ water. Plasmid DNA digestion reactions were prepared using 1µg DNA, 2µl 10X FastDigest buffer, 1 µl restriction enzyme (each), 1 µl FastAP and miliQ water up to 20µl.

DNA ligations were performed using Rapid DNA ligation kit (Thermo Scientific). Ligations were incubated overnight at room temperature. Ligated DNA inserts were cloned into plasmids and then sequenced.

2.2.6 Transformation of chemically competent *E. coli* cells

E. coli competent cells were prepared according to the Rubidium Chloride protocol (Sambrook J, 1989). Shortly, cells were diluted 1:100 in LB from an overnight culture and grown at 37ºC to an early exponential phase (OD_{550nm} 0.3-0.4). The cultures were placed on ice for 15 min and centrifuged at 3,500 rpm for 20 min at 4ºC. The pellet was resuspended in 100 ml of ice-cold RF1 buffer (12g/L RbCl; 9.9g/L $MnCl_2 \cdot 4H_2O$; 30 mM KAc, pH 5.8; 1.5g/L $CaCl_2$; 15% Glycerol). After incubation on ice for 15 min and centrifugation at 3,500 rpm for 15 minutes at 4ºC, the pellet was resuspended in 50 ml ice-cold RF2 buffer (10 mM MOPS; .12 g/L $RbCl_2$; 11g/L $CaCl_2$; Glycerol 15%). Competent cells were separated in 100 µL aliquots, snap frozen in liquid nitrogen and stored at -80ºC. For transformation, chemically competent cells were thawed on ice and incubated with either plasmid DNA or ligation mixtures for 15 min. Cells were heat shocked at 42ºC for 1 min and immediately after, cells were incubated on ice for 5 min and rescued in 1ml LB. Cells recovered for 1h at 37ºC with shaking and 100 µl cells suspension was plated on LA supplemented with ampicillin (100µg/ml), while the remaining was centrifuged (10,000 rpm, 3 min) and suspended in 100 µl LB before platting on the same media .

2.2.7 Transformation of electrocompetent *S. aureus* cells

S. aureus RN4220 competent cells were prepared as previously described (Kraemer and Iandolo, 1990). Shortly, cells were diluted 1:200 into 100 ml fresh medium (TSB) from an overnight culture and grown at 37ºC with aeration until an OD_{600} of 0.4-0.6. Cells were then harvested by centrifugation (8000 rpm for 15 minutes at 4ºC) and washed with 100 ml of ice-cold 0.5M sucrose solution (filter sterilized), harvested at 4ºC and resuspended in 50ml of ice-cold 0.5M sucrose solution. After incubation on ice for 15 min, cells were harvested at 4ºC and resuspended in 300 µl of sucrose 0.5M. Cells in 50 µl aliquots were quickly frozen in liquid nitrogen and stored at -80ºC.

Competent *S. aureus* cells were then transformed by electroporation with plasmid DNA. For that purpose, 50µl cells were thawed on ice. Exceptionally, for FtsZ plasmids, the volume of cells was doubled (2x50 µl) in order to increase the number of transformants Therefore, the 1st aliquot of cells was centrifuged for 10 sec at 4°C and the pellet was used to resuspend the 2nd aliquot. 5 µl or 10 µl plasmid DNA was added to the cells, transferred to a 0.2cm Gene Pulser cuvette (BioRad), and incubated on ice for 5 min. Cells were electroporated by applying a pulse at 2.5kV, 25 µF and 100 Ω in a Gene Pulser apparatus (BioRad). Cells were immediately recovered in 1 ml TSB and incubated at 37ºC with aeration for 1h or 30ºC for 1h30. 100 µl cells was plated on TSA supplemented with appropriate antibiotics and the remaining volume was

harvested (10,000 rpm for 3 min), resuspended in 100 µl fresh medium (TSB) and plated out on the same media. Plates were incubated at 30ºC or 37ºC overnight.

2.2.8 Transduction of *S. aureus* cells

S. aureus strains were transduced with plasmid DNA using phage 80α, according to previously described methods (Oshida and Tomasz, 1992). In order to do that, a lysate of the donor strains was prepared. Firstly, 20 mL bottom phage agar (casamino acids 3 g/L, Difco; yeast extract 3g/L, Difco; NaCl 5.9 g/L, Sigma; agar 15 g/L, Difco; pH 7.8) plates and 3 mL phage top agar (casamino acids 3 g/L, Difco; yeast extract 3g/L, Difco; NaCl 5.9 g/L, Sigma; agar 5 g/L, Difco; pH 7.8) test tubes were prepared, both supplemented with 5mM $CaCl_2$. Test tubes were transferred to a 55°C waterbath for at least 1h. For generation of the phage lysate, a full 10 µl loops with confluent growth of the donor strain was suspended in 500 µl TSB supplemented with 5mM $CaCl_2$. The 80α phage lysate was diluted from 10^{-1} to 10^{-7} in phage buffer ($MgSO_4$ 1mM, $CaCl_2$ 4 mM, Tris-HCl 50 mM pH 7.8, NaCl 5.9 g/L, gelatin 1 g/L). 10 µl of diluted lysate (10^0, 10^{-2}, 10^{-4}, 10^{-6}, and 10^{-7}) was added to 10 µl of the cell suspension before pipetting the mixture into the phage top agar, slightly swirling and pouring immediately onto the Bottom agar plate. After settled, the agar plates were incubated at 30°C overnight. The next day, the plates with confluent lysis were incubated with 3ml of phage buffer at 4°C for 1h. The mixture was collected into a 50ml falcon tube and disrupted by vortexing. The falcon tube was incubated at 4ºC for 1h, so that the phage in the phage agar is allowed to be transferred to the phage buffer, and centrifuged (3,000 rpm for 15 min) to sediment the top agar. The supernatant was filtered using a 0.45 µm sterile filter and lysate was stored at 4°C for subsequent transduction. To test lysate sterility, 50 µl of phage lysate was plated on TSA and incubated at 37°C overnight.

For transduction, 10ml 0,3GL bottom agar (casamino acids 3g/L, Difco; yeast extract 3g/L, Difco; NaCl, 5.9g/L, Sigma; sodium lactate 60% syrup, 3.3ml/L, Sigma; glycerol 50% (v/v), 2ml/L, Sigma; Tri-sodium citrate, 0.5g/L, Sigma; and agar 15g/L, Difco; pH 7,8) plates containing 3x the concentration of antibiotic used for selection (Erm 30µg/mL(Sigma); Kan and Neo 150 µg/mL or Cm 30 µg/mL) were prepared. Additionally, 3ml 0,3GL Top agar (casamino acids 3g/L, Difco; yeast extract 3g/L, Difco; NaCl, 5.9g/L Sigma; sodium lactate 60% syrup, 3.3ml/L, Sigma; glycerol 50% (v/v), 2ml/L, Sigma; Tri-sodium citrate, 0,5g/L, Sigma; and agar 7,5g/l, Difco; pH 7,8) test tubes were incubated at 55ºC for at least 1h. Plates were allowed to set and 20 ml 0,3GL bottom agar without antibiotics was added to each plate, which was used within one hour. A cell suspension of the recipient *S. aureus* strain was made by collecting 2 full 10 µl loops with confluent growth into 1ml TSB supplemented with 5mM $CaCl_2$. Different volumes of phage lysate (0.2 µl, 1µl, 10 µl, 100 µl) were added to tubes containing 100 µl cell suspension and 100 µl phage buffer supplemented with 5 mM $CaCl_2$. As a negative control, no phage lysate was added to the mixture.

Transduction mixtures were placed at 37°C for 20 min with shaking before being transferred to 3ml 0,3GL top agar test tubes, which were slightly swirled and immediately poured onto the 0,3GL plates. Settled plates were incubated at 37°C or 30°C for 48h.

2.3 Construction of plasmids and strains

2.3.1 Construction of *split-gfp$_{p7}$* fusions to gene of interest

All plasmids and bacterial strains used in this study are indicated in **Tables 2.2** and **2.3** respectively. For generation of *split-gfp$_{p7}$* fragments, a region containing the first 462-bp of the *gfp$_{p7}$* gene (5'*gfp$_{p7}$*) and a region containing the last 252-bp of *gfp$_{p7}$* (3'*gfp$_{p}$*) were obtained by PCR from pBCB30, a plasmid that contains *gfp$_{p7}$*, in order to produce N-terminal and C-terminal GFP$_{P7}$ fragments, respectively. Our genes of interest, namely *ftsZ, ezrA*, *pbp2* and *pbp4*, were amplified by PCR from *S. aureus* COL genomic DNA and joined either to 5'*gfp$_{p7}$* or to 3'*gfp$_{p7}$* fragments.

Table 2.1 – Primers used in this study

Primer	Sequence 5' – 3'[a]
pBCBseqfor	GGTAGCCCTTGCCTACCTAGC
pBCBseqrev	GTAAGATTTAAATGCAACCG
pCNseqUPfw	CATATCAGGCAGATAATC
pCNseqDWRev2	CAAAATTATACATGTCAACG
PepsaSeqFW2	AGATATCTCGGACCGTC
Ppepsaii	GCGTTTCACTTCTGAG
UpSpa(800bp) For	CGAAGTTAAAATGGAAAAGTG
DownSpa(800 bp) Rev	CCTTGCAGATCAAAGTGAATC
SmaI-RBS-FtsZ For	GCCCGGGAAAAAATAAGGAGGAAAAAAAATGTTAGAATTTGAACAAG G
FtsZ-linker-BamHI Rev	GCCGGATCCGCCAGAGGCGGAACCTCCACGTCTTGTTCTTCTTGAAC
BamHI-linker-C-GFP For	GCCGGATCCGCTTCGGGAGGCTCAGCATCGGACAAACAAAAGAATGG AATC
C-GFP-XhoI Rev	GGCGCTCGAGTTATTTGTATAGTTCATCCATGCCATG
BamHI-linker-N-GFP For	GCCGGATCCGCTTCGGGAGGCTCAGCATCGAGTAAAGGAGAAGAACT TTTC
N-GFP-XhoI Rev	GGCGCTCGAGTTATGCCATGATGTATACATTGTGTG
PstI-RBS-EzrA For	GGCTGCAGAAAAAAtAAGGAGGAAAAAAAATGGTGTTATATATCATTT TG
EzrA-linker-BamHI Rev	GCCGGATCCGCCAGAGGCGGAACCTCCTTGCTTAATAACTTCTTCTTC
C-GFP-KpnI Rev	CCGGTACCTTATTTGTATAGTTCATCCATGCCATGTG
N-GFP-KpnI Rev	CCGGTACCTTATGCCATGATGTATACATTGTGTGAG
PstI-RBS-PBP4 For	GGCTGCAGAAAAAATAAGGAGGAAAAAAAATGAAAAATTTAATATCT ATTATC
PBP4-linker-BamHI Rev	GCCGGATCCGCCAGAGGCGGAACCTCCTTTTCTTTTTCTAAATAAAC
SacI-RBS-N-GFP For	GCGGAGCTCAAAAAATAAGGAGGAAAAAAAATGAGTAAAGGAGAAG AAC

N-GFP-linker-BamHI Rev	GCCGGATCCGCCAGAGGCGGAACCTCCTGCCATGATGTAT ACATTGTG
BamHI-linker-PBP2 For	GCCGGATCCGCTTCGGGAGGCTCAGCATCGACGGAAAACAAAGGATC TTC
PBP2-SalI Rev	GCGGTCGACTTAGTTGAATATACCTGTTAATCCACCGC
EzrA (600bp) For	GCGCACAACCATATAGC
PBP2 (600bp) For	CTATTCTGATGGCGTAAC
FtsZ (500bp) For	CAAATGACCGTTTATTAG
PBP4 (600bp) For	GTATAAAGACCAAGAAC
PBP2 (800bp) Rev	CTGTTTATCTGTAATGC
PstI-RBS-C-GFP For	GGCTGCAGAAAAAAtAAGGAGGAAAAAAAATGGACAAACAAAAGAAT GGAATC
LacI_Seq_P1	GGCGATGGCGGAGCTGAATTAC
LacI For	ATGAAACCAGTAACGTTATAC
pMADII	CGTCATCTACCTGCCTGGAC
pMADI	CTCCTCCGTAACAAATTGAGG
spa-_P1_BamHI	TGAGGATCCCCAGGCTTGTTGTTGTCTTC
spa-_P4_NCOI	TGCAGTCCATGGTTGAAAAAGAAAAACATTTATTC

[a] Restrictions sites are underlined.

Table 2.2 – Plasmids used in this study

Plasmids	**Relevant genetic characteristics**	**Source or Reference**
pCNX	*E. coli*-S. *aureus* shuttle vector; replicative in *S. aureus*; Amp^r Kan^r Neo^r; Cadmium-inducible P_{cad} promoter;	Monteiro *et al*., 2015
pEPSA	*E. coli*-S. *aureus* shuttle vector; replicative in *S. aureus*; Amp^r,Cm^r; Xylose-inducible P_{xyl} promoter, XylR	(Forsyth *et al*., 2002)
pBCB13	*E. coli*-S. *aureus* shuttle vector*;* integrative in *S. aureus*; Amp^r Erm^r; IPTG-inducible P_{spac} promoter	Pereira *et al*., 2010
pBCB30	*S. aureus* integrative vector containing gfp_{P7} gene;	Laboratory strain (unpublished)
pCNX-PBP4-C-GFP_{P7}	*E. coli*-S. *aureus* shuttle vector; replicative in *S. aureus*; encoding a C-terminal PBP4-C-GFP_{P7} fusion; Kan^r, Neo^r	This study
pCNX-EzrA-C-GFP_{P7}	*E. coli*-S. *aureus* shuttle vector; replicative in *S. aureus*; encoding a C-terminal EzrA-C-GFP_{P7} fusion; Kan^r, Neo^r	This study
pCNX-EzrA-N-GFP_{P7}	*E. coli*-S. *aureus* shuttle vector; replicative in *S. aureus;* encoding a C-terminal EzrA-N-GFP_{P7} fusion; Kan^r, Neo^r	This study
pEPSA-N-GFP_{P7}-PBP2	*E. coli*-S. *aureus* shuttle vector; replicative in *S. aureus*; encoding a N-terminal N-GFP_{P7}-PBP2 fusion; Cm^r	This study

pEPSA-N-GFP$_{P7}$	*E. coli*-S. *aureus* shuttle vector; replicative in *S. aureus*; encoding N-terminal GFP$_{P7}$ fragment; Cm^r	This study
pCNX-C-GFP$_{P7}$	*E. coli*-S. *aureus* shuttle vector; replicative in *S. aureus*; encoding C-terminal GFP$_{P7}$ fragment; Kan^r, Neo^r	This study
pBCB13-FtsZ-C-GFP$_{P7}$	*E. coli*-S. *aureus* shuttle vector; integrative in *S. aureus;* encoding a C-terminal FtsZ-C-GFP$_{P7}$ fusion; Erm^r	This study
pBCB13-FtsZ-N-GFP$_{P7}$	*E. coli*-S. *aureus* shuttle vector; integrative in *S. aureus;* encoding a N-terminal FtsZ-C-GFP$_{P7}$ fusion; Erm^r	This study
pCNX-C-GFP$_{mut1}$	*E. coli*-S. *aureus* shuttle vector; replicative in *S. aureus*; encoding C-terminal GFP$_{mut1}$ fragment; Kan^r, Neo^r	Laboratory strain (N. Reichmann and M.G. Pinho, unpublished)
pEPSA-N-GFP$_{mut1}$	*E. coli*-S. *aureus* shuttle vector; replicative in *S. aureus*; encoding N-terminal GFP$_{mut1}$ fragment; Cm^r	Laboratory strain (N. Reichmann and M.G. Pinho, unpublished)

Table 2.3 – Bacterial strains used in this study

Strains	**Relevant genetic characteristics**	**Source or Reference**
E. coli		
DC10B	Δ*dcm* in the DH10B background; Dam methylation only	Monk *et al*., 2012
S. aureus		
NCTC8325-4	MSSA strain	R.Novick
RN4220	Restriction-deficient derivative of NCTC8325-4	R.Novick
COL	HA-MRSA strain	Gill *et al*., 2005
RNspa::P$_{spac}$-GFP	RN4220 expressing GFP at the *spa* locus under the control of P$_{spac}$	Laboratory strain (unpublished)
RNpCNX-PBP4-C-GFP$_{P7}$	RN4220 with pCNX-PBP4-C-GFP$_{P7}$ plasmid encoding C-terminal GFP$_{P7}$ fragment fused to PBP4; Kan^r, Neo^r	This study
RNpCNX-EzrA-C-GFP$_{P7}$	RN4220 with pCNX-EzrA-C-GFP$_{P7}$ plasmid encoding C-terminal GFP$_{P7}$ fragment fused to EzrA; Kan^r, Neo^r	This study
RNpCNX-EzrA-N-GFP$_{P7}$	RN4220 with pCNX-EzrA-N-GFP$_{P7}$ plasmid encoding C-terminal GFP$_{P7}$ fragment fused to EzrA; Kan^r, Neo^r	This study
RNpCNX	RN4220 with pEPSA; Kan^r, Neo^r	This study
RNspa::FtsZ-C-GFP$_{P7}$	RN4220 with integrated FtsZ-C-GFP$_{P7}$ fusion at the *spa* locus encoding C-terminal GFP$_{P7}$ fragment fused to FtsZ; Erm^r	This study

RNspa::FtsZ-N-GFP_{P7}	RN4220 with integrated FtsZ-N-GFP_{P7} fusion at the *spa* locus encoding N-terminal GFP_{P7} fragment fused to FtsZ; Erm^r	This study
RNpEPSA-N-GFP_{P7}-PBP2	RN4220 with pEPSA-N-GFP_{P7}-PBP2 plasmid encoding N-terminal GFP_{P7} fragment fused to PBP2; Kan^r, Neo^r	This study
RNpEPSA	RN4220 with pEPSA; Cm^r	This study
RNpEPSA-N-GFP_{P7}-PBP2 pCNX-PBP4-C-GFP_{P7}	RNpEPSA-N-GFP_{P7}-PBP2 with pCNX-PBP4-C-$GFP_{P7;}$ expressing N-GFP_{P7}-PBP2 and PBP4-C-GFP_{P7} fusions; Kan^r, Neo^r Cm^r	This study
RNspa::FtsZ-C-GFP_{P7} pCNX-EzrA-N-GFP_{P7}	RNspa::FtsZ-C-GFP_{P7} with pCNX- EzrA-N-$GFP_{P7;}$ expressing FtsZ-C-GFP_{P7} fusion and EzrA-N-GFP_{P7} fusion; Kan^r, Neo^r	This study
RNspa::FtsZ-N-GFP_{P7} pCNX-EzrA-C-GFP_{P7}	RNspa::FtsZ-N-GFP_{P7} with pCNX- EzrA-C-$GFP_{P7;}$ expressing FtsZ-N-GFP_{P7} fusion and EzrA-C-GFP_{P7}; Kan^r, Neo^r	This study
RNspa::FtsZ-C-GFP_{P7} pEPSA-N-GFP_{P7}-PBP2	RNspa::FtsZ-C-GFP_{P7} with pEPSA-N-GFP_{P7}-PBP2; expressing FtsZ-C-GFP_{P7} fusion and N-GFP_{P7}-PBP2; Cm^r	This study
RNpEPSA-N-GFP_{P7}-PBP2 pCNX-EzrA-C-GFP_{P7}	RNpEPSA-N-GFP_{P7}-PBP2 with pCNX-EzrA-C-$GFP_{P7;}$ expressing N-GFP_{P7}-PBP2 and EzrA-C-GFP_{P7}fusions; Kan^r, Neo^r Cm^r	This study
RNpEPSA-N-GFP_{P7}	RN4220 with pEPSA encoding N-terminal GFP_{P7} fragment ; Cm^r	This study
RNpCNX-C-GFP_{P7}	RN4220 with pCNX encoding C-terminal GFP_{P7} fragment ; Kan^r, Neo^r	This study
RNpCNX-C-GFP_{P7} pEPSA-N-GFP_{P7}	RNpCNX-C-GFP_{P7} with pEPSA-N-GFP_{P7}; expressing C-GFP_{P7} and N-GFP_{P7} fusions; Kan^r, Neo^r Cm^r	This study
RNpCNX-PBP4-C-GFP_{P7} pEPSA-N-GFP_{P7}	RNpCNX-PBP4-C-GFP_{P7} with pEPSA-N-$GFP_{P7;}$ expressing PBP4-C-GFP_{P7} and N-GFP_{P7} fusions; Kan^r, Neo^r Cm^r	This study
RNpCNX-C-GFP_{P7} pEPSA-N-GFP_{P7}-PBP2	RNpCNX-C-GFP_{P7} with pEPSA-N-$GFP_{P7;}$ expressing C-GFP_{P7} and N-GFP_{P7} fusions; Kan^r, Neo^r Cm^r	This study
RNpCNX-C-GFP_{mut1} pEPSA-N-GFP_{mut1}	RNpCNX-C-GFP_{mut1} with pEPSA-N-GFP_{mut1}; expressing C-GFP_{P7} and N-GFP_{mut1} fusions; Kan^r, Neo^r Cm^r	Laboratory strain (N. Reichmann and M.G. Pinho, unpublished)

2.3.1.1 Construction of *ftsZ-c-gfp$_{p7}$* and *ftsZ-n-gfp$_{p7}$* fusions

In order to fuse the C-terminal fragment of GFP_{p7} to FtsZ, two DNA fragments were produced. A truncated fragment consisting of the last 27-bp of the region encoding the $(GGSAS)_3$ linker and the 3'*gfp$_{p7}$* gene with the stop codon were amplified from pBCB30 using primer pair BamHI-linker-C-GFP For/ C-GFP-XhoI Rev. A second fragment, which contains the ribosome binding site (RBS), the initiation codon (ATG), the integral *ftsZ* gene and the first 24-bp of the region encoding the $(GGSAS)_3$ linker was generated by amplifying *ftsZ* from *S. aureus* COL genome with primer pair SmaI-RBS-FtsZ For/ FtsZ-linker-BamHI Rev. Both PCR fragments were digested with BamHI, ligated and then joined in a second PCR (overlap PCR), using primer pair SmaI-RBS-FtsZ For/C-GFP-XhoI Rev. The final PCR product was digested with SmaI/XhoI restriction enzymes and cloned into an integrative plasmid, pBCB13, which has a thermosensitive origin for replication at 30ºC and can be integrated in bacterial chromosome at 43ºC (Pereira *et al*., 2010).

To create a C-terminal fusion in which FtsZ was fused to the N-terminal fragment of $GFP_{p7,}$ a fragment consisting of the last 27-bp of the region encoding the $(GGSAS)_3$ linker and the 5'*gfp$_{p7}$*, were amplified using primer pair BamHI-linker-N-GFP For/ N-GFP-XhoI Rev. A second fragment, containing the RBS, the ATG codon, the integral *ftsZ* gene and the first 24-bp of the region encoding the $(GGSAS)_3$ linker was amplified with primer pair SmaI-RBS-FtsZ For/ FtsZ-linker-BamHI Rev. Once again, resulting PCR fragments were digested with BamHI, ligated and then joined in an overlap PCR, using primer pair SmaI-RBS-FtsZ For/N-GFP-XhoI Rev. The final insert was cloned into pBCB13 vector at SmaI and XhoI restriction sites. The resulting plasmids, pBCB13-FtsZ-N-GFP_{P7} and pBCB13- FtsZ-C-GFP_{P7}, were used to transform *E. coli DC10B*. Plasmids were confirmed to be present by colony screening using pBCB13 specific primers (pBCBseqfor/ pBCBseqrev). Prior to sequencing, a restriction digestion was performed in order to confirm inserts correct orientation (Table A.1, Appendix). After sequencing, correct pBCB13 FtsZ-N-GFP_{P7} and pBCB13-FtsZ-C-GFP_{P7} plasmids were electroporated into *S. aureus* strain RN4220, resulting in RNpBCB13-FtsZ-N-GFP_{P7} and RNpBCB13-FtsZ-C-GFP_{P7} strains, respectively. Transformants were selected in TSB supplemented with Erm (10µg/ml) at 30ºC and presence of plasmids was confirmed by colony screening using pBCB13 specific primers.

For integration of the plasmids into RN4220 chromosome, colonies were grown overnight in TSB supplemented with Erm at 30ºC. The culture was diluted 1:1000 in the same medium and grown at 30ºC for 8h for plasmid replication. This culture was re-diluted 1:1000 in the same medium as before and incubated at 43ºC for 16h, so that plasmid replication does not occur. The overnight culture was diluted 1:10 in TSB and dilutions 10^{-4}, 10^{-5} and 10^{-6} were plated in TSB supplemented with Erm and X-Gal at 43ºC. Blue colonies were selected and patched on the same medium for incubation at 43ºC. Integration of pBCB13

fusion plasmids at the *spa* locus was confirmed by PCR. For that purpose, a plasmid specific primer and a chromosome specific primer were used, namely UpSpa(800bp)/C-GFP XhoI-rev or UpSpa(800bp)/pBCB13seqrev primer pairs to confirm pBCB13-FtsZ-C-GFP$_{P7}$ integration into the chromosome or pMADII/Spa-p4_NcoI to confirm pBCB13 FtsZ-N-GFP$_{P7}$ integration. Recombination takes place via the upstream (UPspa) or downstream (DOWNspa) regions of the *spa* gene locus (Pereira *et al*., 2010). The resulting PCR products revealed integration at the 5'end of *spa* locus (UPspa). Clones containing the integrated plasmids were grown overnight in TSB at 43ºC for stocking or 30ºC to proceed for excision.

To allow excision of the plasmids integrated into RN4220 chromosome, a second recombination event should occur through UPspa or DOWNspa, generating one of two situations (Pereira *et al*., 2010). If recombination occurs through UPspa, *spa* gene will remain in the chromosome giving rise to RN4220 WT colonies, but if it occurs via DOWNspa, *spa* will be excised together with the plasmid, and the fusion of interest (construct) will remain in the chromosome, producing mutant colonies. Thus, the overnight culture was diluted 1:1000 into TSB and inoculated at 30ºC for 8h. Subsequently, culture was back-diluted 1:10 in TSB and dilutions 10^{-4}, 10^{-5} and 10^{-6} were platted on TSA supplemented with X-Gal at 43ºC. In this stage, white and blue colonies appeared on plate, which represent colonies in which excision had occurred and colonies in which integrated plasmid has not been excised. White colonies represent either mutant or WT colonies. Thereby, white colonies were patched on TSA supplemented with X-Gal at 37ºC and colonies that remained white were selected and patched on TSA supplemented with X-Gal and Erm at 37ºC. To confirm that replacement of the *spa* gene by the *ftsZ-c-gfp*$_{p7}$ and *ftsZ-n-gfp*$_{p7}$ constructs was successful, Erm susceptible colonies were screened by PCR using primer pairs LacI_Seq_p1/ DownSpa (800bp) rev and Upspa(800bp) For/ C-GFP XhoI Rev. The resulting strains, containing *ftsZ-c-gfp*$_{p7}$ and *ftsZ-n-gfp*$_{p7}$ fusions at the *spa* locus of RN4220 chromosome, under the control of P_{spac} promoter, were named RNspa::FtsZ-C-GFP$_{P7}$ and RNspa::FtsZ-N-GFP$_{P7}$, respectively.

2.3.1.2 Construction of *ezrA-c-gfp*$_{p7}$ and *ezrA-n-gfp*$_{p7}$ fusions

Firstly, a fragment containing the RBS, the ATG, *ezrA* integral gene and the first 24-bp of the region encoding the $(GGSAS)_3$ linker was amplified from COL genomic DNA by using primer pair PstI-RBS-EzrA For/ EzrA-linker-BamHI Rev. Then, *gfp*$_{p7}$ was amplified from pBCB30 using primer pairs BamHI-linker-C-GFP For/ C-GFP-KpnI Rev or BamHI-linker-N-GFP For/ N-GFP-KpnI Rev, to generate 5' *gfp*$_{p7}$ or 3' *gfp*$_{p7}$ fragments, respectively. In order to generate a fragment in which 3' *gfp*$_{p7}$ is fused to the 3' end of *ezrA*, the PCR product resulted from the first PCR and 3' *gfp*$_{p7}$ fragment were digested with BamHI, ligated and joined by overlap PCR using primer pair PstI-RBS-EzrA For/ C-GFP-KpnI Rev. On the other hand, to produce a fragment in which 5' *gfp*$_{p7}$ is fused to the 3' end of *ezrA*, PCR products of *ezrA* and 3' *gfp*$_{p7}$ were

also digested, ligated and joined by overlap PCR using primer pair PstI-RBS-EzrA For/ N-GFP-KpnI Rev. Both PCR products were restricted digested with PstI and KpnI enzymes, producing 1.5 kb and 1.7 kb inserts, that were subsequently cloned into a multi-copy vector, pCNX (Monteiro *et al*., 2015) into PstI and KpnI sites. The resulting plasmids, pCNX-EzrA–C-GFP$_{P7}$ and pCNX-EzrA-N-GFP$_{P7}$, were transformed into *E.coli* DC10B, restricted digested to confirm inserts orientation (Table A.1, Appendix) and sequenced. Then, plasmids were electroporated into RN4220, giving rise to strains RNpCNX-EzrA-C-GFP$_{P7}$ and RNpCNX-EzrA–N-GFP$_{P7}$, in which *ezrA-c-gfp$_{p7}$* and *ezrA-n-gfp$_{p7}$* fusions were both placed under the control of P$_{cad}$ promoter.

2.3.1.3 Construction of *pbp4–c-gfp$_{p7}$* fusion

The *ppb4* gene was amplified from COL genomic DNA by using primer pair PstI-RBS-PBP4 For/ PBP4-linker-BamHI Rev, generating a fragment which contains the RBS, the ATG codon, *pbp4* gene and the first 24-bp of a region encoding the (GGSAS)$_3$ linker. A second fragment that contains the last 27-bp of the region encoding the same linker in frame with 3' *gfp$_{p7}$* was obtained, using primer pair BamHI-linker-C-GFP For/ C-GFP-KpnI Rev. In order to join both PCR fragments, immediately after digesting fragments at the BamHI sites and ligating, an overlap PCR was performed by using primer pair PstI-RBS-PBP4 For/ C-GFP-KpnI Rev. The resulting PCR product, a 1.6 kb insert, was digested and cloned into PstI and KpnI restriction sites of pCNX vector, resulting in pCNX-PBP4-C-GFP$_{P7}$ plasmid. After transforming DC10B strain, plasmid was confirmed by restriction digestion (Table A.1, Appendix) and sequenced. The correct plasmid was then moved to RN4220 by electroporation, giving rise to RNpCNX-PBP4-C-GFP$_{P7}$ strain. This strain expresses the *c-gfp$_{p7}$-pbp4* under the control of *P$_{cad}$* promoter.

2.3.1.4 Construction of *n-gfp$_{p7}$-pbp2* fusion

The *pbp2* gene was amplified from COL genome by using primer pair BamHI-linker-PBP2 For/PBP2-SalI Rev. The resulted fragment contains the last 27-bp of the region encoding the (GGSAS)$_3$ linker and the integral *pbp2* gene. In order to obtain the *gfp$_{p7}$* gene, a region containing the RBS, followed by the 3'*gfp$_{p7}$* with the ATG codon, and the first 24-bp of the region encoding the same linker was amplified from pBCB30 by using primer pair SacI-RBS-N-GFP For/ N-GFP-linker-BamHI Rev. The resulting DNA fragments were digested with BamHI, ligated and joined in an overlap PCR using primer pair SacI-RBS-N-GFP For/ PBP2-SalI Rev, producing a 2.7kb insert. This insert was then digested with SacI and SalI restriction enzymes and cloned into a multi-copy vector, pEPSA. Following DC10B transformation and digestion to confirm insert (Table A.1, Appendix), plasmid was sequenced. The correct plasmid, named

pEPSA-N-GFP$_{P7}$-PBP2, was then electroporated into RN4220, giving rise to RNpEPSA-N-GFP$_{P7}$-PBP2 strain, which contains *n-gfp$_{p7}$-pbp2* fusion, under the control of P_{xyl} promoter.

2.3.1.5 Construction of *n-gfp$_{p7}$* fusion

A fragment of 498-bp containing the RBS, the ATG codon and 5' *gfp$_{p7}$* was amplified from pBCB30 by using primer pair SacI-RBS-N-GFP for for/N-GFP KpnI rev. The amplification product contains SacI and KpnI restriction sites, used for cloning of the insert into pEPSA, downstream of the xylose-inducible P_{xyl} promoter. The resulting plasmid, named pEPSA-N-GFP$_{P7}$ was used to transform DC10B strain and restriction digestion was performed in order to confirm insert orientation. After sequencing, plasmid was electroporated into RN4220, resulting in strain RNpEPSA-N-GFP$_{P7}$, which expresses *n-gfp$_{p7}$* fusion, encoding the N-terminal fragment of GFP$_{P7}$, under the control of P_{xyl} promoter.

2.3.1.6 Construction of *c-gfp$_{p7}$* fusion

A fragment of 291-bp containing the RBS, the ATG codon and 3'*gfp$_{p7}$* was amplified from pBCB30 by using primer pair PstI-RBS-C-GFP for/ C-GFP-KpnI Rev. The same cloning procedure was made as for the construct described in section 2.3.1.5 The resulting plasmid, named pCNX-C-GFP$_{P7}$ was transformed into DC10B, confirmed by restriction digestion and sequenced. The correct plasmid was introduced into RN4220 by electroporation, giving rise to RNpCNX-C-GFP$_{P7}$. This final strain expresses C-terminal fragment of GFP$_{P7}$ under the control of P_{cad} promoter.

2.3.2 Construction of *S. aureus* strains expressing two fusions

The previously constructed strains, contain plasmids expressing one of four proteins of interest, FtsZ, EzrA, PBP2 or PBP4, attached either to the N- or the C-terminal fragments of GFP$_{P7}$.

To produce a strain that expresses both fusions of interest encoding for proteins that putatively interact, a set of phage transductions, described below, was performed.

2.3.2.1 Strain expressing FtsZ and EzrA fusions

To construct a strain co-expressing FtsZ and EzrA in fusion with a GFP$_{P7}$ fragment, a phage lysate of RNpCNX-EzrA-N-GFP$_{P7}$ was prepared (see 2.2.8) for extraction transduction of the plasmid DNA. The strain RNspa::FtsZ-C-GFP$_{P7}$ (see 2.3.1.1) was infected with the generated phage lysate, allowing for

transduction with pCNX EzrA-N-GFP$_{P7}$ (see 2.3.1.2) plasmid, resulting in RNspa::FtsZ-C-GFP$_{P7}$ pCNX EzrA-N-GFP$_{P7}$. The final strain expresses FtsZ-C-GFP$_{P7}$ protein fusion under the control of an IPTG-inducible promoter, P_{spac}, and EzrA-N-GFP$_{P7}$ fusion under the control of a cadmium-inducible, P_{cad}. A similar procedure was made to produce RNspa::FtsZ-N-GFP$_{P7}$ pCNX EzrA-C-GFP$_{P7}$ strain. This strain expresses FtsZ-N-GFP$_{P7}$ and EzrA-C-GFP$_{P7}$ fusions under the control of P_{spac} or P_{cad} promoters, respectively.

2.3.2.2 Strain expressing PBP2 and PBP4 fusions

In order generate a strain that expresses both PBP2 and PBP4 fusions to GFP$_{P7}$, a phage lysate of strain RNpEPSA-N-GFP$_{P7}$-PBP2 (see 2.3.1.4) was prepared in order to enable transduction of pEPSA-N-GFP$_{P7}$-PBP2 plasmid into RNpCNX-PBP4-C-GFP$_{P7}$ (see 2.3.1.3), giving rise to RNpCNX-PBP4-C-GFP$_{P7}$ pEPSA-N-GFP$_{P7}$-PBP2 strain. The resulted strain contains N-GFP$_{P7}$-PBP2 and PBP4-C-GFP$_{P7}$ fusions, expressed under the control of either a xylose-inducible promoter (P_{xyl}) or a cadmium-inducible (P_{cad}) promoter, respectively.

2.3.2.3 Strains expressing PBP2 and EzrA or PBP2 and FtsZ fusions

In order to construct a strain that contains GFP$_{P7}$ fragments fused either to PBP2 and EzrA or to PBP2 and FtsZ, pEPSA-N-GFP$_{P7}$-PBP2 (see 2.3.1.4) plasmid was introduced either into RNspa::FtsZ-C-GFP$_{P7}$ (see 2.3.1.1) or into RNpCNX-EzrA-C-GFP$_{P7}$ (see 2.3.1.2) strains by transduction. The final strains were named i) RNspa::FtsZ-C-GFP$_{P7}$ pEPSA-N-GFP$_{P7}$-PBP2, expressing FtsZ-C-GFP$_{P7}$ and N-GFP$_{P7}$-PBP2 fusions under the control of P$_{spac}$ promoter or under the control of P$_{xyl}$ promoter; and ii) RNpCNX-EzrA-C-GFP$_{P7}$ pEPSA-N-GFP$_{P7}$-PBP2, expressing EzrA-C-GFP$_{P7}$ and N-GFP$_{P7}$-PBP2 fusions under the control of the same promoters as strain described in i).

2.3.2.4 Strain expressing N-GFP$_{P7}$ and C-GFP$_{P7}$ fusions

To produce a strain that contains both *n-gfp$_{p7}$* and *c-gfp$_{p7}$* fusions pEPSA-N-GFP$_{P7}$ plasmid (see 2.3.1.5) was transduced into RNpCNX-C-GFP$_{P7}$ strain (see 2.3.1.6). The resulted strain, named RNpCNX-C-GFP$_{P7}$ pEPSA-N-GFP$_{P7}$, expresses proteins fusions under the control of P$_{cad}$ promoter (C-GFP$_{P7}$) or under the control of P$_{xyl}$ promoter (N-GFP$_{P7}$).

2.3.2.5 Strains expressing C-GFP$_{P7}$ and N-GFP$_{P7}$-PBP2 fusions or N-GFP$_{P7}$ and PBP4-C-GFP$_{P7}$ fusions

To obtain split-GFP$_{P7}$ fusions to only PBP2 or PBP4, two different strains were produced. For that purpose, pEPSA-N-GFP$_{P7}$-PBP2 plasmid (2.3.1.4) was introduced into RNpCNX-C-GFP$_{P7}$ strain (see 2.3.1.6) by transduction, giving rise to RNpCNX-C-GFP$_{P7}$ pEPSA-N-GFP$_{P7}$-PBP2. This strain expresses C-GFP$_{P7}$ fusion under the control of P_{cad} promoter and N-GFP$_{P7}$-PBP2 fusion, under the control of P_{xyl} promoter. Likewise, pEPSA-N-GFP$_{P7}$ (see 2.3.1.5) was transduced into RNpCNX-PBP4-C-GFP$_{P7}$ (see 2.3.1.3) resulting in RNpCNX-PBP4-C-GFP$_{P7}$ pEPSA-N-GFP$_{P7}$ strain. This strain expresses an N-GFP$_{P7}$ fusion under the control of P_{xyl} promoter and a PBP4-C-GFP$_{P7}$ fusion, under the control of P_{cad} promoter.

2.4 Fluorescence microscopy

For fluorescence microscopy experiments, *S. aureus* RN4220 strains were grown overnight in TSB at 37ºC with appropriate antibiotic selection. Cells were diluted 1:200 in fresh TSB (without antibiotic) and inducers were added to the cultures as follows; 0.1µM cadmium chloride ($CdCl_2$) for strains containing *pbp4* and *ezrA* fusions under the control of P_{cad} promoter, 0.5mM IPTG for strains with *ftsZ* fusions under the control of P_{spac} promoter and 0.05% xylose for strain with *pbp2* fusions under the control of P_{xyl} promoter. When growth has reached an OD_{600} of 0.75-0.8, 1ml of culture was pelleted and resuspended in 16 µl of 1X phosphate-buffered saline (PBS). 1µl of cell suspension was placed onto a thin layer of 1.2% agarose in PBS. Phase-contrast and fluorescence images were captured using a Zeiss Axio Observer.Z1 fluorescence microscope equipped with a Plan-Apochromat objective (100x/1.4 Oil Ph3; Zeiss) and a Photometrics CoolSNAP HQ2 camera (Roper Scientific). GFP fluorescence was measured by excitation at 485 and emission at 510 nm. Exposure time was typically 500ms. All images were acquired using ZEN 2012 software (Carl Zeiss).

2.5 Fluorescence quantification and statistical analysis

Fluorescence images were analyzed using ImageJ software (Abramoff, M.D, 2004). For this purpose, the mean fluorescence per pixel of each cell was measured, in at least 100 cells per strain. This value was corrected by subtracting the mean background fluorescence. This way, corrected fluorescence intensity for each strain was determined. For strains without fluorescence at the septum, cytoplasmic

fluorescence was measured by drawing a circle a slightly smaller than the cell and recording the mean fluorescence. As for strains with fluorescent signal at the septum, only cells with a closed septum were considered for quantification, through one of two methods. The first method consisted in measuring fluorescence intensity at the septum by drawing a polygon section around this area, while in the second method fluorescence intensity is measured in three distant points (at the center and in the borders) of the closed septum.

Further statistical analysis of data included unpaired t – tests for comparison of corrected cell fluorescence intensity values among strains.

3. RESULTS

3.1 GFP_{P7} split-site selection

In this study we used an improved version of GFP, superfast GFP or GFP_{P7}, which contains several mutations that enhance its folding properties and increase its fluorescence signal (Fisher and DeLisa, 2008). Previous work with BiFC systems has used eYFP (Hu *et al*., 2002; Soufo and Graumann, 2006; Pazos *et al*., 2013). According to Hu and colleagues eYFP (enhanced version of YFP) contains three mutations relatively to YFP: S65G, S72A, T203Y (Hu *et al*., 2002).

We have analyzed the sequences of GFP_{P7} and eYFP fluorescent proteins and identified seven point mutations relatively to eYFP: F64L, G65A, N105Y, E124V, Y145F, Y203T, and L231H. (**Fig.3.1B**). Some of these mutations correspond to the mutation sites that were used to improve GFP_{P7} relatively to a non-engineered GFP (GFP_{mut2})(Fisher and DeLisa, 2008).

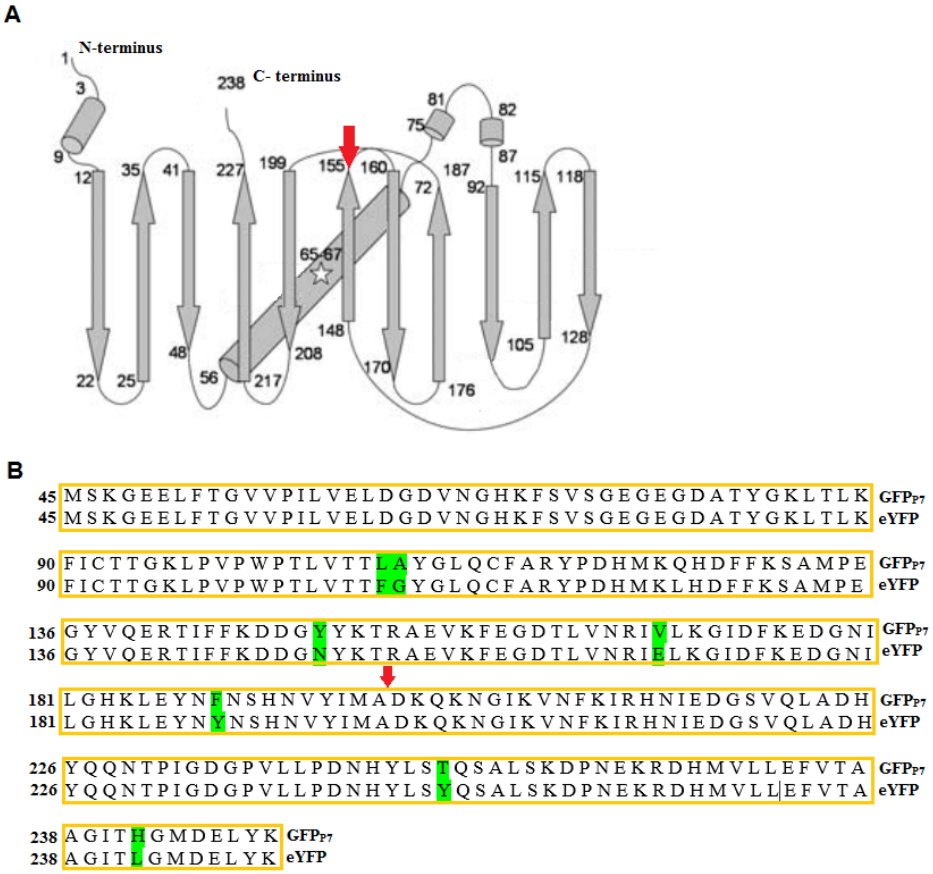

Figure 3.1 GFP_{P7} split-site selection based on GFP_{P7} topology and sequence comparison with YFP. A) A schematic representation of GFP topology shows the split-site: between7th and 8th β-strands at residue 154, producing an N-terminal fragment of 154 amino acids and a C-terminal fragment of 84 amino acids. The three amino acid residues

(65-67) that compose the fluorophore remain intact. The arrow (red) indicates GFP_{P7} split-site. B) Sequence analysis has revealed 7 mutation sites (shown in green) between GFP_{P7} and YFP sequences. The arrow (red) represents GFP_{P7} split-site. Fig. (B) adapted from Fisher and DeLisa, 2008.

Circular permutation studies have identified that splitting GFP in a region between 7th and 8th β-strands should not affect its structure and, thus its ability reconstitute the fluorophore (Kodama and Hu, 2012). Moreover, eYFP-based studies which had split eYFP into two fragments, between amino acids residues 154 and 155, had successfully detected protein-interactions (Hu *et al*., 2002; Soufo and Graumann, 2006; Pazos *et al*., 2013). According to these reports, and since GFP_{P7} and eYFP sequences did not show major differences between both proteins (**Fig.3.1**), splitting GFP_{P7} in the same position as eYFP should generate similar results. Therefore, we split GFP_{P7} between 7th and 8th β-strands, in order to produce an N-terminal fragment (N-GFP_{P7}), composed of amino acid residues 1-154 and a C-terminal fragment (C-GFP_{P7}) composed of residues 155-238 (**Fig.3.1A**).

3.2 Choice of type of fusions based on protein topology

Each of the four proteins under study (PBP2, PBP4, EzrA and FtsZ) was fused to either the C-terminal domain or the N-terminal domain of GFP_{P7}. Details of the constructed fusions are described below. **Figure 3.2** shows a schematic representation of constructs that were produced and their relative sizes.

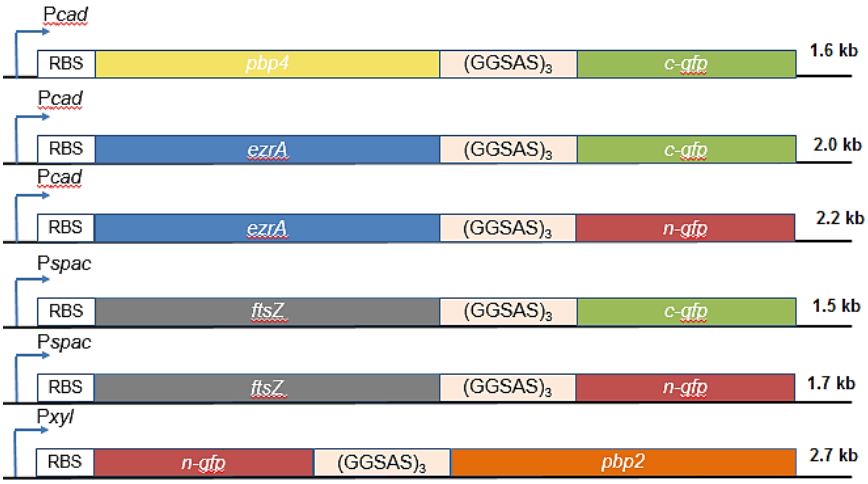

Figure 3.2 – Schematic representation of the constructed fusions and respective sizes. The resulted protein fusions, except FtsZ fusions, were overexpressed from different plasmids, under control of different promoters. FtsZ fusions were expressed under the control of an inducible promoter, from an integrative plasmid for integration into the genome. Therefore, it is possible to control their expression levels.

This choice of the type of fusions was based on the protein topology in the cell and localization of its C-terminal and N-terminal domains. GFP is not properly folded when localized outside of the cytoplasm (Feilmeier *et al*., 2000). To maintain GFP_{P7} fragments in the cytoplasm, they should be linked to the cytoplasmic domains of the putative interacting proteins. PBP2 N-terminal domain is located at the cytoplasm, linked to a transmembrane anchor, while C-terminal TGase domain is at the outer surface of the cell membrane, linked to a TPase domain by a β-rich linker (Lovering *et al.*, 2007). In turn, PBP4 N-terminal TPase domain is at the outer surface of the membrane while the C-terminal all-β domain is localized in the cytoplasm (Navratna *et al*., 2010). Therefore, it is reasonable to construct a fusion where the N-terminal fragment of GFP_{p7} is fused to the N-terminal domain of PBP2 and the C-terminal terminal fragment of GFP_{p7} is attached to the C-terminal domain of PBP4.

FtsZ is a cytosolic protein composed of two domains, arranged around a central helix (H7), an N-terminal domain with GTPase activity and a C-terminal domain that contains a highly conserved core domain, which is important for binding of several cell-division proteins (Löwe and Amos, 1998; Hale and De Boer, 1999; Erickson, 2001). EzrA contains an N-terminal transmembrane anchor and the C-terminal domain is located in the cytoplasm (Adams and Errington, 2009). We have made C-terminal fusions of the N-or C-terminal fragments GFP_{P7} to FtsZ and EzrA.

3.6 Protein interaction studies of single split-GFP_{P7} protein fusions

Based on previous BiFC studies using eYFP, a similar system using GFP_{P7} will be developed. When GFP_{P7} fragments are splitted in strategic sites and fused to putative interacting proteins, if an interaction between such pair of proteins occurs, once they are localized in close proximity to each other, the non-fluorescent GFP_{P7} fragments can associate, restoring GFP_{P7} fluorescence. Moreover, this event enables us to determine at which sub-cellular sites these proteins interact during *S.aureus* cell cycle.

We constructed *in silico* sets of *split-*gfp_{p7} fusions, in which regions encoding the N-terminal or C-terminal fragments of GFP_{p7} where fused N- or C-terminally to genes encoding *S. aureus* chromosomal proteins FtsZ, EzrA, PBP2 and PBP4. Each protein of interest was linked to their respective split-GFP_{P7} fragment via a flexible 15 amino acid linker of $(GGSAS)_3$.

According to previous studies, separate YFP fragments are not fluorescent. Therefore, when a YFP fragments is fused to a single protein and this fusion is expressed alone no fluorescence or very low fluorescence is detected (Hu *et al*., 2002; Soufo and Graumann, 2006). Likewise, when GFP_{P7} fragments are split and fused to a protein, a similar result is expected.

To test this possibility, we constructed strains expressing individually each protein of interest. The resulting strains named, RNpEPSA-N-GFP$_{P7}$-PBP2, RNpCNX-PBP4-C-GFP$_{P7}$, RNspa::FtsZ-C-GFP$_{P7}$, RNspa::FtsZ-N-GFP$_{P7}$, RNpCNX-EzrA-C-GFP$_{P7}$ and RNpCNX-EzrA-N-GFP$_{P7}$, were later analyzed by fluorescence microscopy. For that purpose, overnight cultures were back-diluted 1:200 in TSB and incubated with appropriate inducers. For IPTG-inducible strains (P_{spac} promoter), expressing FtsZ-C-GFP$_{P7}$ and FtsZ-N-GFP$_{P7}$, 0.5mM IPTG was used; for cadmium-inducible strains (P_{cad} promoter), expressing PBP4-C-GFP$_{P7}$, EzrA-C-GFP$_{P7}$ and EzrA-N-GFP$_{P7}$, 0.1 µM $CdCl_2$ was used; and for xylose-inducible strains (P_{xyl} promoter) containing PEPSA-N-GFP$_{P7}$-PBP2, 0.05% xylose was added to the culture. Strains were incubated at 37ºC with aeration and at OD_{600} of ~0.75-0.8 cells were prepared and visualized by microscopy. As described previously, the constructed fusions were cloned either in multi-copy vectors pCNX or pEPSA, except for FtsZ fusions, which were integrated into the chromosome, at the *spa* locus, to have a better control of fusion expression, as FtsZ overexpression compromises cell survival (Lutkenhaus,1992). As negative controls of GFP expression, we used strains containing an empty vector, i.e. which does not express any fusion, RNpCNX or RNpEPSA, and as a positive control we used a strain that expresses a full copy of GFP at the ectopic *spa* locus under the control of P_{spac} promoter, RNspa:: P_{spac} -GFP.

Microscopy analysis of cells expressing FtsZ-C-GFP$_{P7}$, FtsZ-N-GFP$_{P7}$, EzrA-C-GFP$_{P7}$, EzrA-N-GFP$_{P7}$, PBP4-C-GFP$_{P7}$ and N-GFP$_{P7}$-PBP2 revealed that protein fusions (**Fig.3.2D-F, H-J**) produced low GFP$_{P7}$ cytoplasmic fluorescence, when compared to their positive control (**Fig.3.3B**) and identical to their negative controls. (**Fig.3.3D-G**). Therefore, unlike the positive control, expressing a full copy of GFP, these strains were not able to reconstitute the fluorophore.

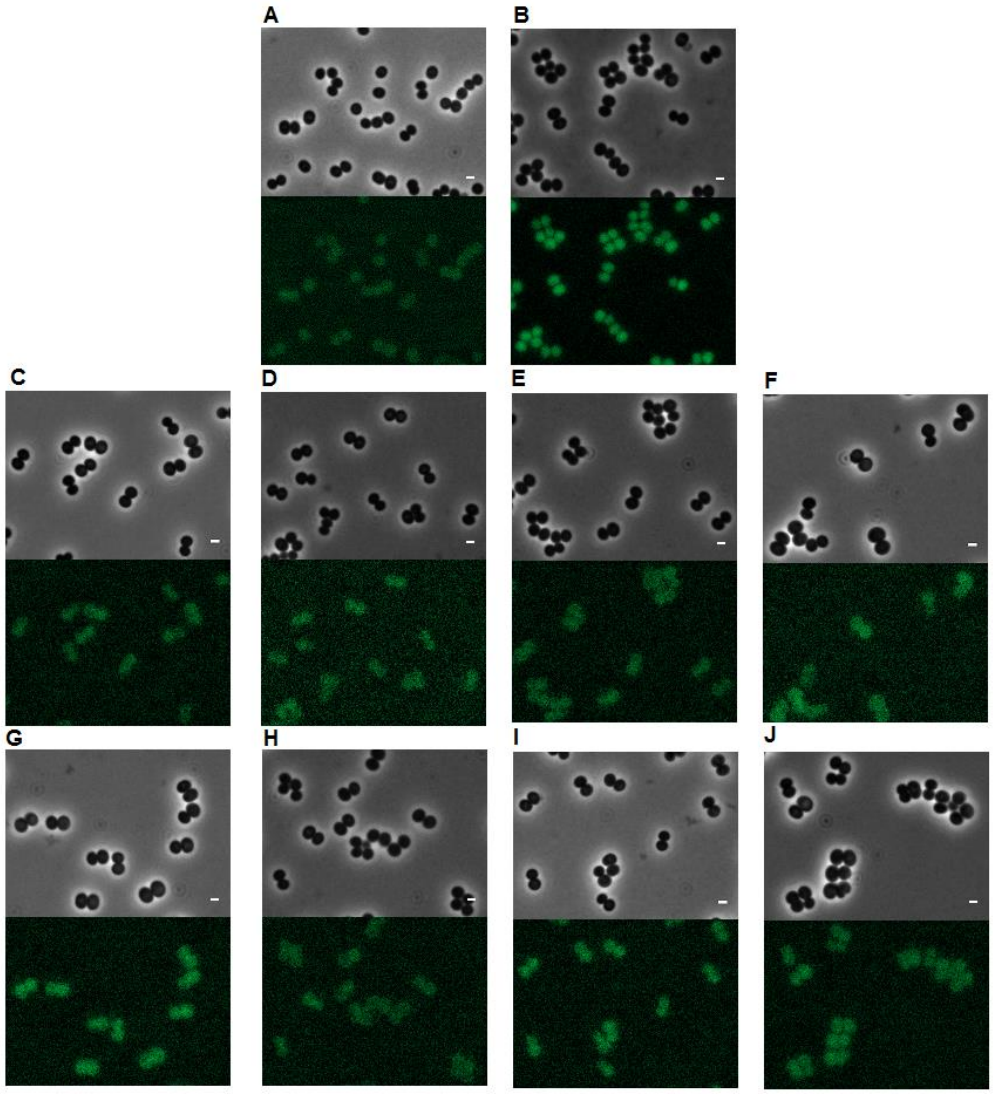

Figure 3.3 Microscopy analysis of cells expressing single split-GFP_{P7} protein fusions. (A) RN4220 WT (B) RNspa:: P_{spac} -GFP, used as positive control for all strains. Strain was grown in presence of 0.5mM IPTG. (C) RNpCNX, used as a negative control for cadmium inducible-strains expressing PBP4-C-GFP_{P7} (D), EzrA-C-GFP_{P7} (E) or EzrA-N-GFP_{P7} (F) fusions. Cells were grown in presence of 0.1µM $CdCl_2$. (G) RNpEPSA, used as a negative control for xylose inducible strain, expressing N-GFP_{P7}-PBP2 (H) fusion. Cells were grown with 0.05% xylose. (I) RN4220 IPTG-inducible strains expressing FtsZ-C-GFP_{P7} (I) and FtsZ-N-GFP_{P7} (J) fusions. Cells were grown in presence of 0.5mM IPTG. Phase-contrast images (top) and GFP fluorescence images (bottom) are shown. Exposure times were 500ms. Scale bar: 1µm.

As GFP_{P7} fragments were shown not to be fluorescent, we then analyzed the levels of auto fluorescence emitted by each strain. Comparison of fluorescence signal resulting from expression of different fusions was determined by fluorescence quantification. The mean fluorescence value of a cell is

defined as the average fluorescence signal of each pixel inside the outlined area. To compare the fluorescence signals produced by each strain, a total of 100 cells (N=100) were analyzed, by drawing a circle slightly smaller than the cells and the mean fluorescence was recorded. The background signal was subtracted to the mean fluorescence value of each cell and a corrected mean fluorescence intensity (CFI) value was obtained. Therefore, CFI value of each strain defines the fluorescence intensity level displayed by each fusion. We have compared CFI for strains in which expression of fusions is under the control of P_{cad}, P_{xyl} or P_{spac} (at the ectopic *spa* locus) (**Fig.3.4**).

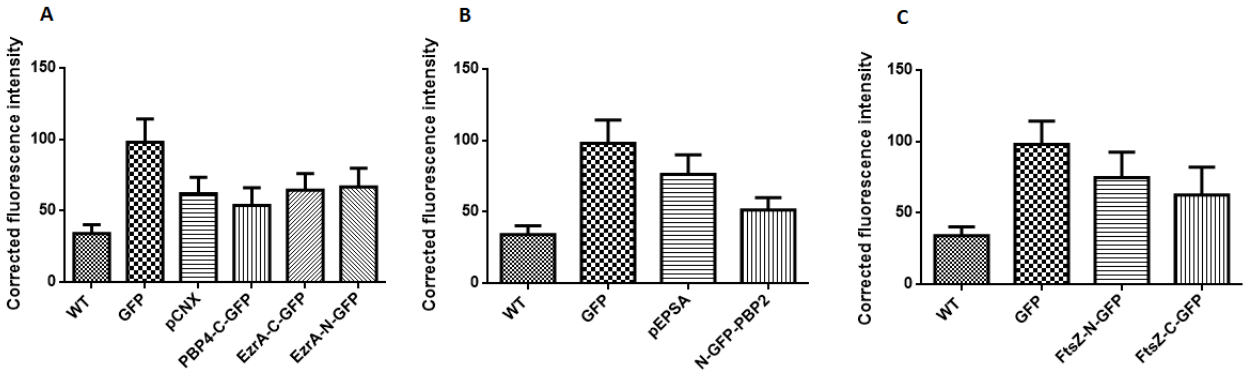

Figure 3.4 Fluorescence quantification of single split-GFP_{P7} fusions. **.** Comparison of corrected mean fluorescence (CFI) between (A) RNpCNX (negative control) and RN4220 cells expressing PBP4-C-GFP, EzrA-C-GFP, EzrA-N-GFP under the control of P_{cad} promoter; (B) RNpEPSA (negative control) and RN4220 cells expressing N-GFP-PBP2 under the control of P_{xyl} promoter; (C) RN4220 cells expressing FtsZ-N-GFP and FtsZ-C-GFP fusions at the *spa* locus, under the control of P_{spac} promoter. All strains were also compared to RN4220 wild-type (WT) and RNspa:: P_{spac}-GFP (GFP), used as a positive control. The mean fluorescence value of a cell is the fluorescence signal of each pixel inside the outlined area subtracted by the background signal. CFI was measured for each cell by drawing a circle around the cell. Data shown as mean± SD; N=100.

3.7 Protein interaction studies of combined split-GFP_{P7} protein fusions

Fragments of YFP truncated at residue 155 have been reported to produce relatively bright fluorescence signals in complexes formed by many interaction partners, but when fused to partners that do not interact, low fluorescence is displayed (Hu *et al.*, 2002; Soufo and Graumann, 2006; Kerppola, 2008). Moreover many controls are needed to demonstrate that signal detected is a result from a specific protein interaction (Kerppola, 2008).

3.7.1 FtsZ-EzrA interaction as a positive control

There is evidence for the interaction between FtsZ and EzrA in *S.aureus*. Besides EzrA localization to the mid-cell being dependent on FtsZ, EzrA is required for divisome assembly and subsequent PG synthesis. (Levin et al, 1999, Steele, Jorge et al 2011). Furthermore, EzrA and FtsZ were proven to interact using a bacterial-two hybrid system and were shown to co-localize at the nascent division site. (Steele *et al*., 2011). Likewise, these proteins are putative good candidates to be used as a positive control in this study. When combined in a split-GFP_{P7} system, if FtsZ and EzrA show an interaction, fluorescence is expected to be detected at the nascent division septum in dividing cells. This observation would enable us to assume that our system is functional and has potential to provide further information about interactions between PBP2 and PBP4.

3.4.2 Analysis of FtsZ-EzrA split-GFP_{P7} fusions

In order to test the functionality of our system, we have generated RN4220 strains expressing both FtsZ and EzrA fusions to the C- or N-terminal GFP_{P7} fragments.

In order to express FtsZ and EzrA fusions simultaneously, we have transduced a multi-copy plasmid expressing EzrA-C-GFP_{P7} under the control of P_{cad} promoter into a strain expressing FtsZ-N-GFP_{P7} at the ectopic *spa* locus, under the control of P_{spac} promoter. Likewise, a plasmid containing EzrA-N-GFP_{P7} fusion was introduced into a strain expressing FtsZ-C-GFP_{P7}. The final strains were grown at 37°C in presence of of 0.5mM IPTG and 0.1 µM $CdCl_2$ until an OD_{600} of ~0.75-0.8. At the desired OD_{600} were harvested and protein interaction studies were performed by fluorescence microscopy (**Fig.3.5.B, D**). Growth in presence of the described concentration of inducers was shown to affect cell growth and shape.

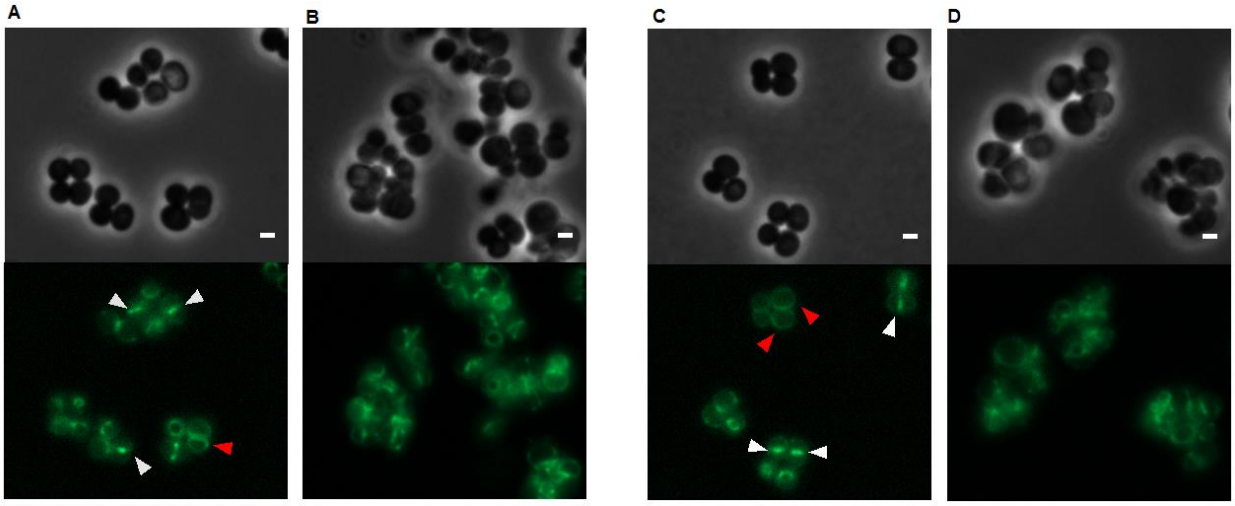

Figure 3.5 Microscopy analysis of cells expressing FtsZ-EzrA split-GFP_{P7} fusions. (A-B) RN4220 cells expressing both FtsZ-C-GFP_{P7}, under the control of P_{spac} promoter, and EzrA-N-GFP_{P7}, under the control of P_{cad} promoter from

a multi-copy plasmid (pCNX). Cells were grown in absence (A) or presence (B) of 0.5mM IPTG and 0.1µM $CdCl_2$. (C-D) RN4220 cells expressing both FtsZ-N-GFP_{P7}, under the control of P_{spac} promoter, and EzrA-C-GFP_{P7} fusion under the control of P_{cad} promoter from pCNX. Cells were grown in absence (C) or presence (D) of 0.5mM IPTG and 0.1µM $CdCl_2$. Phase-contrast images (top) and GFP fluorescence images (bottom) are shown. Arrows in white indicate the formation of a putative protein complex in the division septum (circles or lines across the cells); arrows in red indicate the formation of a putative protein complex around the cell membrane. Exposure times were 500ms. Scale bar: 1µm.

Therefore we decided to incubate these strains at 37°C without inducer and harvest cells at the desired OD_{600} (~0.75-0.8) for visualization of protein interactions (**Fig.3.5A-C**). FtsZ and EzrA have earlier shown to localize simultaneously to the division septum (Steele *et al*., 2011). Accordingly, we observed that FtsZ-C-GFP_{P7} and EzrA-N-GFP_{P7} protein fusions as well as FtsZ-N-GFP_{P7} and EzrA-C-GFP_{P7} fusions, co-localized simultaneously to this place (represented as fluorescent circles or lines across the cells). This is in agreement with the hypothesis that FtsZ and EzrA establish an interaction in *S.aureus* cells. The fluorescence signal, which was not present in strains expressing single split-GFP_{P7} fusions, is restored by association of GFP_{P7} portions.

Importantly, it was observed that even without inducer (**Fig.3.5A-C**) cells are slightly bigger than WT strain and previous mutant strains **(Fig.3.3)**. We assume that protein fusions are not 100% functional and therefore may interfere with the function of native proteins, FtsZ and EzrA. Importantly, EzrA fusions are being expressed in higher number of copies than FtsZ fusions (from a multi-copy vector). It is likely that the activity of this EzrA fusions may be inhibiting the function of the native EzrA. This hypothesis is in concordance with previous observations, in which absence of EzrA led to an increase of the average cell size (Jorge *et al*., 2011; Steele *et al*., 2011). In the presence of inducers, a more severe phenotype, characterized by abnormal cell division is observed (**Fig.3.5B-D**). Formation of a correct Z-ring, essential for cell division in *S.aureus*, is dependent on recruitment of EzrA (Jorge *et al*., 2011). We assume that the overexpression of EzrA interferes with native EzrA and therefore affects FtsZ localization to the mid-cell. It was also observed that in some cells (**Fig. 3.5A-C**) fusion protein delocalizes from the mid-cell and/or is cleaved, as fluorescence is visualized inside the cytoplasm and around the cell membrane.

Once these results give strong indications for the functionality of split-GFP_{P7} system, i.e. that it can be used to visualize proteins interactions, we now will employ it to unravel PBP2 and PBP4 protein interactions in *S.aureus* living cells, which is the main goal of this study.

3.4.3 Analysis of PBP2-PBP4 split-GFP$_{P7}$ fusions

As described previously, two fusions were constructed, a C-terminal fusion of C-terminal GFP$_{P7}$ fragment to PBP4 and an N-terminal fusion of N-terminal GFP$_{P7}$ fragment to PBP2. To generate a strain that contains PBP4-C-GFP$_{P7}$ and N-GFP$_{P7}$-PBP2 fusions, pEPSA-N-GFP$_{P7}$-PBP2 was transduced into RNpCNX-PBP4-C-GFP$_{P7}$. The final strain, RNpCNX-PBP4-C-GFP$_{P7}$ pEPSA-N-GFP$_{P7}$-PBP2, was grown at 37ºC in presence of 0.05% xylose and 0.1 µM $CdCl_2$ until an OD_{600} of ~0.75-0.8 was reached.

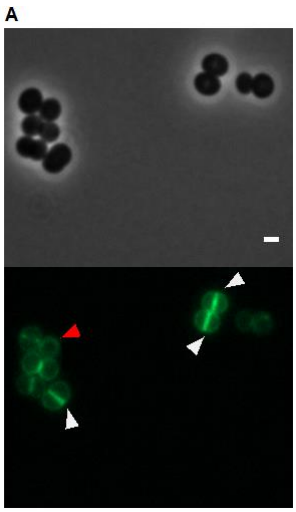

Figure 3.6 Microscopy analysis of cells expressing PBP2-PBP4 split-GFP $_{P7}$ fusions. (A) RN4220 cells expressing PBP4-C-GFP$_{P7}$, under the control of P_{cad} promoter, and N-GFP$_{P7}$-PBP2, under the control of P_{xyl} promoter, both from multi-copy vectors. Cells were grown in presence of 0.05% xylose and 0.1µM $CdCl_2$. Phase-contrast images (top) and GFP fluorescence images (bottom) are shown. Arrows in white indicate the formation of a putative protein complex in the division septum (circles or lines across the cells); arrows in red indicate the formation of a putative protein complex around the cell membrane. Exposure times were 500ms. Scale bar: 1µm.

Microscopy imaging revealed that PBP4-C-GFP$_{P7}$ and pEPSA N-GFP$_{P7}$-PBP2 localize both to the division septum, suggesting that a protein complex between PBP4 and PBP2 is formed in these cells (**Fig.3.6**). However, similarly to what was observed in strains expressing FtsZ and EzrA split-GFP$_{P7}$ fusions, in some cells fusions do not localize only at the septum but also around the cell membrane, suggesting an a additional interaction between PBP2 and PBP4 at this place.

3.4.4 Analysis of PBP2-EzrA and PBP2-FtsZ split-GFP$_{P7}$ fusions

We then decided to take advantage of the constructed fusions to test additional combinations of putative interacting divisome components, namely PBP2 with EzrA and PBP2 with FtsZ. A BTH assay has shown the *S. aureus* divisome to require many pairwise interactions. Importantly, it revealed positive

interactions between PBP2 and EzrA. This finding has led to the hypothesis that EzrA participates not only in Z-ring assembly but also in synthesis of PG (Steele *et al*., 2011). Moreover, it has been reported that in absence of FtsZ, PBP2 is delocalized from the septum and becomes dispersed around the cell membrane. This indicates that PBP2 recruitment to the division septum is dependent on FtsZ (Pinho and Errington ,2003).

To construct a strain that expresses simultaneously PBP2 and FtsZ split-GFP_{P7} fusions, we have transduced pCNX multi-copy plasmid containing N-GFP_{P7}-PBP2 fusion, placed under the control of a xylose inducible promoter (P_{xyl}) into a strain that expresses FtsZ-C-GFP_{P7} from the ectopic *spa* locus, placed under the control of an IPTG-inducible promoter (P_{spac}), giving rise to RNspa::FtsZ-C-GFP_{P7} pEPSA-N-GFP_{P7}-PBP2.

To test for interactions between PBP2 and EzrA, we constructed a strain that expresses both N-GFP_{P7}-PBP2 and EzrA-C-GFP_{P7} fusions. Plasmid pCNX-EzrA-C-GFP_{P7}, containing EzrA-C-GFP_{P7} fusion under the control of P_{cad} promoter was transduced into RNpEPSA-N-GFP_{P7}-PBP2, containing N-GFP_{P7}-PBP2 fusion under the control of P_{spac} promoter. The final strain was named RNpEPSA-N-GFP_{P7}-PBP2 pCNX-EzrA-C-GFP_{P7}.

For expression of proteins fusions, strains expressing FtsZ-C-GFP_{P7} and N-GFP_{P7}-PBP2 was incubated with 0.05 mM IPTG $CdCl_2$ and 0.05% xylose, while strain expressing N-GFP_{P7}-PBP2 and EzrA-C-GFP_{P7} was incubated in presence of 0.05% xylose and 0.1 µM $CdCl_2$. Growth was monitored at 37ºC and at exponential phase (OD_{600} of ~0.75-0.8), cells were harvested and visualized by fluorescence microscopy. When N-GFP_{P7}-PBP2 and EzrA-C-GFP_{P7} fusions were expressed simultaneously, fluorescence was detected at the septum, suggesting that PBP2 and EzrA interact (**Fig.3.7A**), as reported by previous studies. Surprisingly, this phenotype was maintained when N-GFP_{P7}-PBP2 and FtsZ-C-GFP_{P7} fusions were co-expressed (**Fig.3.7B**), suggesting that PBP2 and FtsZ could interact in the divisome.

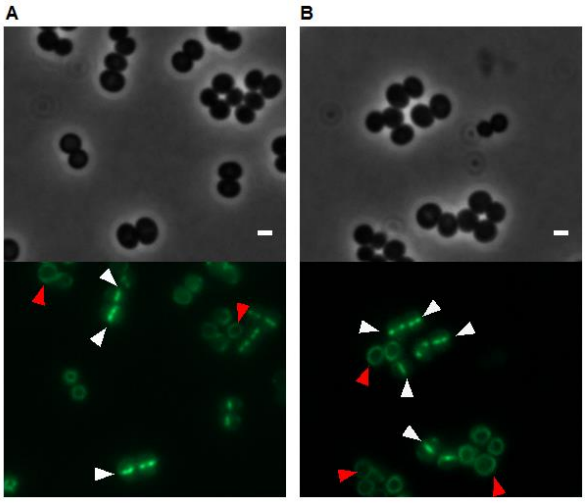

Figure 3.7 Microscopy analysis of cells expressing PBP2-EzrA and PBP2-FtsZ split-GFP $_{P7}$ fusions. (A) RN4220 cells expressing EzrA-C-GFP$_{P7}$, under the control of P_{cad} promoter, and N-GFP$_{P7}$-PBP2, under the control of P_{xyl}, both from multi-copy vectors. Cells were grown in presence of 0.05% xylose and 0.1µM $CdCl_2$. (B) RN4220 cells expressing FtsZ-C-GFP$_{P7}$ at the ectopic *spa* locus, under the control of P_{spac} promoter, and N-GFP$_{P7}$-PBP2, under the control of P_{xyl} from pEPSA. Cells were grown in presence of 0.5 mM IPTG and 0.05% xylose. Phase-contrast images (top) and GFP fluorescence images (bottom) are shown. Arrows in white indicate the formation of a putative protein complex in the division septum (circles or lines across the cells); arrows in red indicate the formation of a putative protein complex around the cell membrane. Exposure times were 500ms. Scale bar: 1µm.

We have then quantified the fluorescence intensity at the septum of each of these strains. Quantification was performed by measuring the fluorescence signal of 100 cells with closed septum (i.e. that show a unique line across the septum) using ImageJ software. Fluorescence at the septum was measured through two different methods.

The first method (Method 1) consisted in measuring fluorescence intensity by outlining a polygon section (rectangle) around the septum area, where the fluorescence is higher, in order to exclude background signal. The mean fluorescence value of a cell corresponds to the fluorescence signal of each pixel inside this area.

The second method (Method 2) consisted in determining fluorescence signal at three points (which represent three pixels) at the septum, including the center and both borders of the cell. Despite method 2 measuring only three pixels in a cell, it reduces the chances of measuring background signal, unlike method 1, which is more susceptible to measure background signal around the outlined septum area. In both methods, the average background signal from five distant points of the image was subtracted to the mean fluorescence value obtained for each cell.

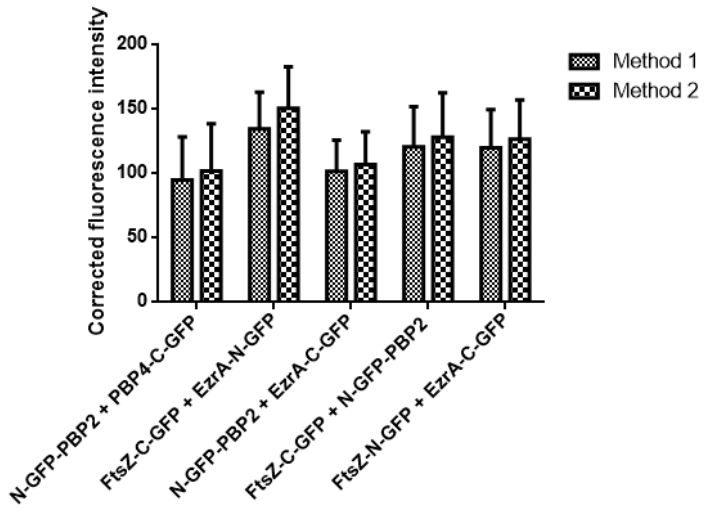

Figure 3.8 Fluorescence quantification of combined split-GFP_{P7} fusions. Comparison of corrected mean fluorescence intensity (CFI) between RN4220 strains expressing: N-GFP-PBP2 and PBP4-C-GFP fusions; FtsZ-C-GFP and EzrA-N-GFP fusions (positive control); N-GFP-PBP2 and EzrA-C-GFP fusions; FtsZ-C-GFP and N-GFP-PBP2 fusions or FtsZ-N-GFP and EzrA-C-GFP fusions (positive control). The mean fluorescence value of a cell is the fluorescence signal of each pixel inside the outlined area subtracted by the background signal. CFI was measured for each cell by drawing a rectangle around the closed septum (method 1) or by recording fluorescence at the 3 points (center and both borders) of the closed septum (method 2). Data shown as mean± SD; N=100.

All of the combinations between putative interacting partners tested were positive. CFI analysis showed higher values using method 2 (**Fig.3.8**). This is reasonable since, as stated above, method 2 excludes most of the background signal, unlike method 1. In each strain, CFI values, and therefore fluorescence intensity, showed some variation within the studied population (100 cells) (represented as high SD values). However, this variation is not significantly different among strains.

3.5 Analysis of additional split-GFP_{P7}fusions

In order for the system to work, GFP_{P7} fragments should not spontaneously associate with each other when they not fused to interacting proteins. When expressed at enough high concentrations, FPs can self-associate (dimerize) with each other (Cabantous *et al*., 2005). Therefore, we found important to eliminate the possibility that FPs self-associate independently from interactions between proteins to which they are fused (Cabantous *et al*., 2005). This event would interfere with the detection of protein interactions, leading to false positive results.

To test if GFP_{P7} fragments do not self-assemble into an intact protein, we have co-expressed both C- and N-terminal fragments of GFP_{P7} unfused to any staphylococcal protein in the same strain. For that

purpose, we started by constructing strains expressing C-GFP$_{P7}$ and N-GFP$_{P7}$ independently from multi-copy plasmids. Therefore, two strains were produced, a strain expressing C-GFP $_{P7}$, under the control of P_{cad} promoter from pCNX and a strain expressing N-GFP, under the control of P_{xyl} promoter from pEPSA. The resulting strains were named RNpCNX-C-GFP and RNpEPSA-N-GFP, respectively. To co-express both fusions in the same strain, pEPSA-N-GFP plasmid was transduced into RNpCNX-C-GFP strain, resulting in RNpCNX-C-GFP pEPSA-N-GFP.

3.5.1 Analysis of C-GFP, N-GFP and C-GFP + N-GFP fusions

Firstly, we have looked at the independent localization of GFP$_{P7}$ fragments in a cell. To induce expression of C-GFP$_{P7}$, RNpCNX-C-GFP was grown in presence of 0.1 µM $CdCl_2$. Likewise, to induce expression of N-GFP$_{P7}$, we added 0.05% xylose to RNpEPSA-N-GFP cells. After growing at 37ºC until an OD_{600} of ~0.75-0.8, cells were harvested and visualized for protein interaction studies.

Microscopy analysis of cells expressing C-GFP$_{P7}$ and N-GFP$_{P7}$ fusions (**Fig.3.9C-D**) revealed that when C-terminal and N-terminal portions of GFP$_{P7}$, unfused to a protein, are independently expressed in RN4220, very low fluorescence is detectable, as previously observed for strains expressing single split-GFP$_{P7}$ fusions (see **Fig.3.3**). Fluorescence at the cytoplasm was quantified as previously described and results confirm microscopy imaging (**Fig.3.10**). When C-GFP$_{P7}$ and N-GFP$_{P7}$ were expressed independently, CFI was lower than for the positive control, expressing a full copy of GFP (RNspa*::*P_{spac}-GFP).

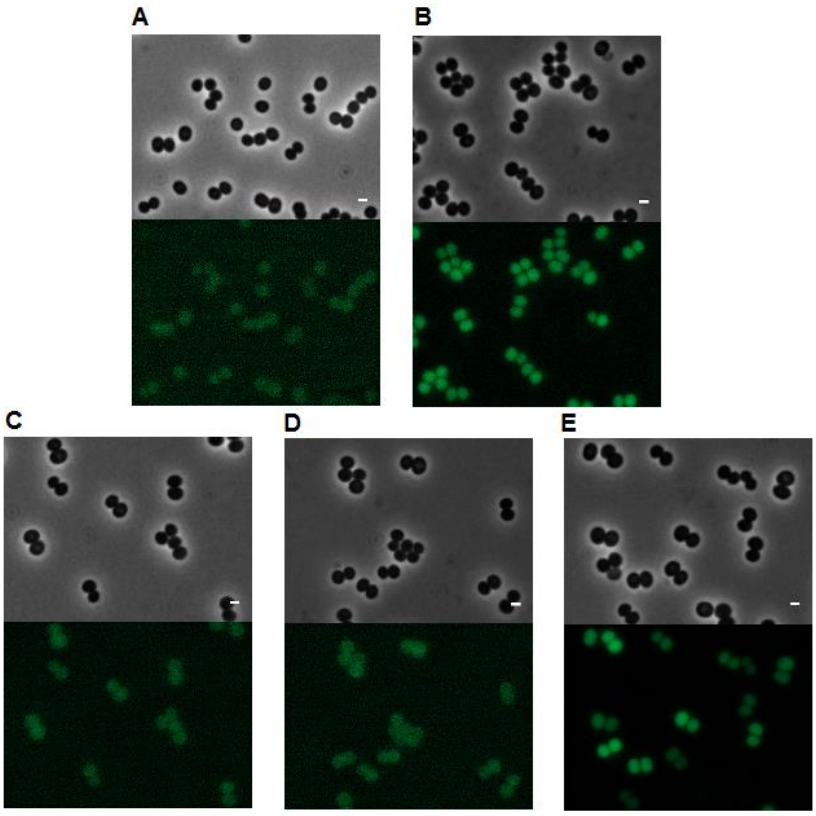

Figure 3.9 Microscopy analysis of cells expressing C-GFP $_{P7}$, N-GFP$_{P7}$ and C-GFP$_{P7}$ + N-GFP$_{P7}$ fusions. (A) RN4220 WT, (B) RNspa:: P_{spac}-GFP, grown in presence of 0.5mM IPTG. (C) RN4220 expressing C-GFP$_{P7}$, under the control of P_{cad} promoter from pCNX; grown in presence of 0.1µM $CdCl_2$. (D) RN4220 expressing N-GFP$_{P7}$, under the control of P_{xyl} from pEPSA; incubated with 0.05% xylose. (E) RN4220 expressing both C-GFP$_{P7}$ and N-GFP$_{P7}$ fusions, incubated with 0.1µM $CdCl_2$ and 0.05% xylose. Phase-contrast images (top) and GFP fluorescence images (bottom) are shown. Exposure times were 500ms. Scale bar: 1µm.

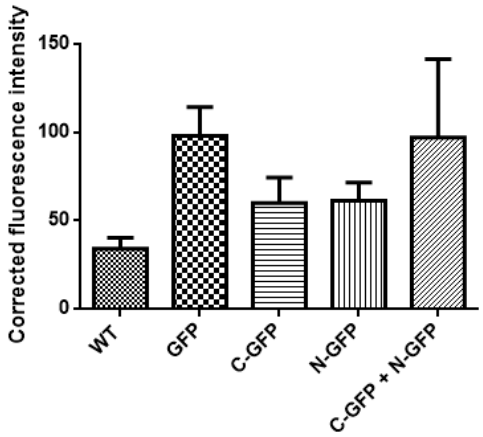

Figure 3.10 Fluorescence quantification of C-GFP, N-GFP and C-GFP$_{P7}$ + N-GFP$_{P7}$ fusions**.** Comparison of corrected mean fluorescence (CFI) between RN4220 strains expressing: C-GFP fusion, N-GFP fusions or both C-GFP and N-GFP fusions and the positive control RNspa:: P_{spac} –GFP. The mean fluorescence value of a cell is the average fluorescence signal of each pixel inside the outlined area subtracted by the background signal. CFI was measured for each cell by drawing a circle around the cell. Data shown as mean± SD; N=100.

To study the simultaneous localization of C-GFP$_{P7}$ and N-GFP$_{P7}$ fusions in a strain, we have grown RNpCNX C-GFP$_{P7}$ pEPSA-N-GFP$_{P7}$ cells at 37ºC in presence of 0.1 µM $CdCl_2$ and 0.05% xylose to an exponential phase ((OD_{600} of ~0.75-0.8). Surprisingly, and contrary to what was reported in the literature for eYFP, (Hu *et al*., 2002; Soufo and Graumann, 2006; Pazos *et al*., 2013) microscopy imaging has shown that fragments of GFP$_{P7}$, C-GFP$_{P7}$ and N-GFP$_{P7}$, can interact and therefore restore cytoplasmic fluorescence (**Fig.3.9E)**, as it was observed for the positive control (RNspa*::P_{spac}-GFP*) (**Fig.3.9)**. These results are supported by fluorescence quantification (**Fig.3.10**) as fluorescence between RN4220 strain expressing C-GFP$_{P7}$ and N-GFP$_{P7}$ fragments and RN4220 expressing GFP$_{P7}$ is very similar, proving that GFP$_{P7}$ fluorescence is restored. However, fluorescence of GFP$_{P7}$ varies from cell to cell as it may depend on the amount of C-GFP$_{P7}$ and N-GFP$_{P7}$ copies in a cell.

3.5.2 Analysis of C-GFP$_{P7}$ + N-GFP$_{P7}$-PBP2 and N-GFP$_{P7}$ + PBP4-C-GFP$_{P7}$ fusions

To confirm the ambiguity of split- GFP$_{P7}$ system we have constructed strains that express both C-GFP$_{P7}$ and N-GFP$_{P7}$ protein fusions, in which one of both fragments of GFP$_{P7}$ is fused to a protein of interest, either PBP2 or PBP4. In order to do that, a plasmid containing N-GFP$_{P7}$-PBP2 fusion (pEPSA-N-GFP$_{P7}$-PBP2) was transduced into a strain expressing C-GFP$_{P7}$ (RNpCNX-C-GFP$_{P7}$), resulting in strain RNpCNX-C-GFP$_{P7}$ pEPSA-N-GFP$_{P7}$-PBP2. Additionally, a plasmid containing PBP4-C-GFP$_{P7}$ fusion (pCNX-PBP4-C-GFP$_{P7}$), was transduced into a strain expressing N-GFP$_{P7}$ (RNpEPSA-N-GFP$_{P7}$), producing strain RNpEPSA-N-GFP$_{P7}$ pCNX-PBP4-C-GFP$_{P7}$. Expression of protein fusions was made by growing both resulting strains at 37ºC in presence of 0.1µM $CdCl_2$ and 0.05% xylose to an exponential phase (OD_{600} of ~0.75-0.8). The phenotype of these strains is determinant as it will give information about previous positive results between the putative interacting proteins.

Co-expression of N-GFP$_{P7}$ and PBP4-C-GFP$_{P7}$ fusions revealed fluorescence signal with localization to the division septum (**Fig.3.11A)**. These results confirm that GFP$_{P7}$ fragments are able of self-association, independently from being fused to a protein or no. Surprisingly, when C-GFP$_{P7}$ and N-GFP$_{P7}$-PBP2 were co-expressed, they localized to the cytoplasm instead of the division septum (**Fig.3.11B**). This may be due to cleavage of the N-GFP$_{P7}$-PBP2, with release of N-GFP$_{P7}$ to the cytoplasm.

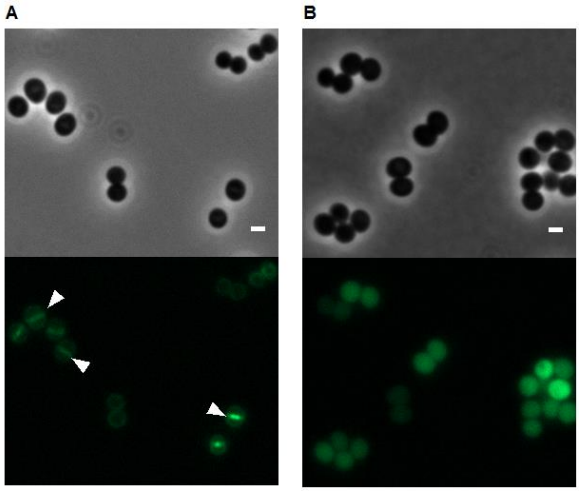

Figure 3.11 Microscopy analysis of cells expressing N-GFP$_{P7}$ + PBP4-C-GFP$_{P7}$ and C-GFP$_{P7}$ + N-GFP$_{P7}$-PBP2 fusions. (A) RN4220 expressing N-GFP$_{P7}$, under the control of P_{xyl} promoter, and PBP4-C-GFP$_{P7}$, under the control of P_{cad}, from multi-copy vectors. Cells were grown in presence of 0.05% xylose and 0.1µM $CdCl_2$. (B) RN4220 expressing C-GFP$_{P7}$, under the control of P_{cad} promoter, or N-GFP$_{P7}$-PBP2, under the control of P_{xyl} promoter. Phase-contrast images (top) and GFP fluorescence images (bottom) are shown. Arrows indicate the places where a putative protein complex is formed (mainly at the division septum). Exposure times were 500ms. Scale bar: 1µm.

3.5.3 Analysis of C-GFP$_{mut1}$ + N-GFP$_{mut1}$ fusions

We have confirmed that split-GFP system using GFP$_{P7}$ is not a reliable method to detect protein interactions, as GFP$_{P7}$ fragments can self-associate into an intact protein. We suggest that, as this protein exhibits enhanced folding properties, it is also more stable than non-improved GFP versions, and therefore their fragments have high affinity to each other and interact. Accordingly, the use of a non-improved version of GFP, which folds at lower rates, may overcome this limitation. To test this possibility, we split GFP$_{mut1}$ between the same amino acid residues as GFP$_{P7,}$ to produce C- and N-terminal fragments of GFP$_{mut1.}$ These fragments, C-GFP $_{mut1}$ and N-GFP$_{mut1}$, were introduced in a strain, as previously described for strain expressing both C-GFP$_{P7,}$ and N-GFP $_{P7}$ fragments, giving rise to strain RNpCNX C-GFP$_{mut1}$ pEPSA N-GFP$_{mut1.}$ We compared this strain with the previous described strain, RNpCNX C-GFP$_{P7}$ pEPSA N-GFP$_{P7,}$ which is able to restore GFP fluorescence. Preliminary microscopy and quantification data has revealed that GFP$_{mut1}$ fragments do not seem to interact to each other, because GFP fluorescence is not restored **(Fig.3.12, Fig.3.13)**. Moreover, RNpCNX C-GFP$_{mut1}$ pEPSA N-GFP$_{mut1.}$shows a similar phenotype to strains expressing single split-GFP$_{P7}$ fusions and their negative controls (**Fig.3.3**). These observations suggest that GFP$_{mut1}$, unlike GFP$_{P7,}$ may be a powerful tool for the interaction of protein-interactions, although a positive control is absolutely essential to confirm if the method is likely to work.

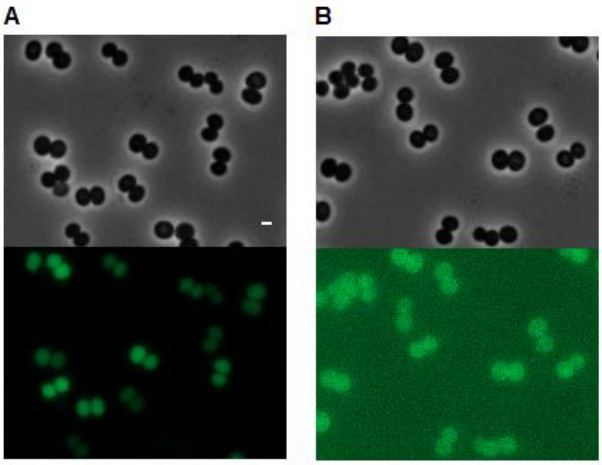

Figure 3.12 Microscopy analysis of cells expressing C-GFP$_{P7}$ + N-GFP$_{P7}$ fusions and C-GFP$_{mut1}$ + N-GFP$_{mu1}$ fusions. (A) RN4220 expressing C-GFP$_{P7}$, under the control of P_{cad} promoter and N-GFP$_{P7}$, under the control of P_{xyl} promoter (B) RN4220 expressing C-GFP$_{mut1}$, under the control of P_{cad} promoter and N-GFP$_{mut1}$, under the control of P_{xyl} promoter. Both strains were grown in presence of 0.1µM $CdCl_2$ and 0.05% xylose. Phase-contrast images (top) and GFP fluorescence images (bottom) are shown. Exposure times were 500ms. Scale bar: 1µm.

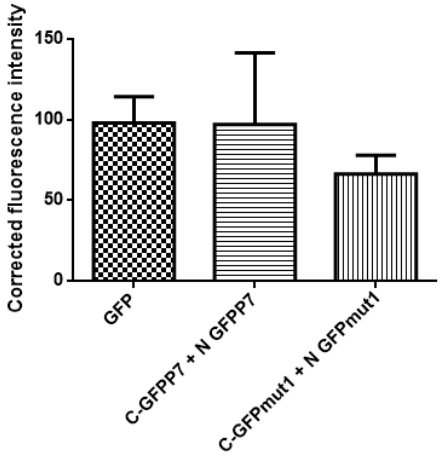

Figure 3.13 Fluorescence quantification of C-GFP$_{mut1}$ + N-GFP$_{mut1}$ fusions. Comparison of corrected mean fluorescence (CFI) between RN4220 strains expressing: C-GFP$_{P7}$ and N-GFP$_{P7}$ fusions (improved GFP) or C-GFP$_{mut1}$ and N-GFP$_{mut1}$ fusions (non-improved GFP) and the positive control (RNspa:: P_{spac} –GFP), expressing a full copy of GFP. The mean fluorescence value of a cell is the average fluorescence signal of each pixel inside the outlined area subtracted by the background signal. CFI was measured for each cell by drawing a circle around the cell. Data shown as mean± SD; N=100.

4. DISCUSSION

PBP2 and PBP4 play major roles in *S. aureus* cell wall synthesis, cell division and antibiotic resistance. PBP4 function has been associated with secondary cross-linking of PG (Wyke *et al*., 1981; Leski and Tomasz, 2005) and resistance to β-lactams in CA-MRSA strains (Memmi *et al*., 2008), whereas PBP2 is involved in cell wall synthesis, being essential for growth and survival of *S. aureus* strains and playing an important role in β-lactam resistance (Pinho *et al*., 2001a; Pinho *et al*., 2001b; Pinho and Errington, 2003). Importantly, loss of PBP2 and PBP4 causes a decrease in susceptibility of *S. aureus* to vancomycin (Sieradzki *et al*., 1999; Sieradzki and Tomasz, 1997). Moreover, PBP2 and PBP4 cooperate in building a highly cross-linked cell wall, upon challenging with antibiotics (Leski and Tomasz, 2005). These findings suggest that these proteins, together with other cell components, are part of a cell wall synthesis machinery that is responsible for the resistance phenotypes in MRSA strains.

In the present study, we aimed to identify an *in vivo* interaction between putative interacting partners PBP2 and PBP4 of *S. aureus*. For that purpose we employed Split-GFP system, using an improved version of GFP, GFP_{P7}. This system is a similar approach to the BiFC assay, originally described in *E. coli* (Hu *et al*., 2002) and later described in *B. subtilis* (Soufo and Graumann, 2006). It is based on the capacity of GFP fragments to spontaneously reassemble when fused to interacting proteins, allowing the detection of transient protein-protein interactions.

To validate our split-GFP_{P7} system we created split-GFP_{P7} fusions to known interacting proteins FtsZ and EzrA, which were used as a positive control. We have observed that FtsZ and EzrA split-GFP_{P7} fusions form a fluorescent complex at the division septum (**Fig.3.5**), suggesting an interaction between these proteins, as reported by previous studies. Furthermore, our proteins of interest, PBP2 and PBP4, were shown to localize at the septum (**Fig.3.6**), suggesting a positive interaction. For strains that expressed split-GFP_{P7} fusions to protein partners that showed positive interactions (FtsZ-EzrA, PBP2-PBP4, PBP2-EzrA-PBP2-FtsZ) fluorescence was detected not only at the division septum, but also (in most of the cases) around the cell membrane. This is unexpected as it implies that these protein partners interact at the cell membrane, which was not previously reported. Nevertheless, only cells with a closed septum were considered for fluorescence quantification. Cells with no detectable fluorescence were rare, initially suggesting that the system was sensitive in detecting protein interactions. Cases in which fluorescence was not detectable, can result either from conformation constraints of split-GFP_{P7} fusions or, most probably, because proteins interact at different phases of the cell cycle.

Fluorophore fragments should only be able to self-assemble and reconstitute the fluorophore, when proteins to which they are fused interact (Hu *et al*., 2002). As every combination of proteins tested has led to positive results, we examined the occurrence of false positives. Therefore, we have constructed a strain

expressing simultaneously N-GFP$_{P7}$ and C-GFP$_{P7}$ fusions. The phenotype of this strain would indicate if the fluorescence displayed by strains combining different interacting partners is a result of one of two events: i) Protein partners interact with each other, leading to N-GFP$_{P7}$ and C-GFP$_{P7}$ association; ii) Non-fluorescent GFP$_{P7}$ fragments self-assemble to form a functional fluorophore, independent from the fact that proteins to which they are fused interact. If event i) did happen we would assume that the system is reliable, as GFP$_{P7}$ association is mediated by an interaction between proteins partners; if event ii) was true, then it would indicate that system is not reliable, as N-GFP$_{P7}$ and C-GFP$_{P7}$ association interferes with the detection of protein interactions. Surprisingly, we observed that when C-GFP$_{P7}$ and N-GFP$_{P7}$ fusions are simultaneously expressed in a strain, fluorescence is detected at the cytoplasm (**Fig.3.9E**), as a result of association between GFP$_{P7}$ fragments. Fluorescence intensity of this strain, resulting from reconstitution of GFP$_{P7}$ is similar to strain expressing a functional GFP$_{P7}$ (**Fig.3.10**). These results demonstrate that our system follows case ii), implying that the septal localization observed in strains expressing combined split-GFP$_{P7}$ fusions (**Fig.3.5-3.7**) is an experimental artifact.

We deduce that GFP$_{P7}$ association does not necessarily result from interactions between protein partners but instead, is a consequence of self-assembly of GFP$_{P7}$ fragments, having led to false positive results. Moreover, we hypothesize that GFP$_{P7}$ fragments are "sticky", as they have high affinity to each other. Once again, this explains fluorescence observed in strains expressing combined split-GFP$_{P7}$ fusions and the septal fluorescence shown when PBP4-C-GFP$_{P7}$ and N-GFP$_{P7}$ fusions were simultaneously expressed. This last strain expresses PBP4, in the absence of an interacting partner, but fluorescence is detected at the septum (**Fig.3.11A**). However, as there is no partner to interact with PBP4, only background signal should be detected, as for strain containing a single PBP4-C-GFP$_{P7}$ fusion (**Fig.3.3C**). Therefore, the septal fluorescence is a result from PBP4 localization, due to GFP$_{p7}$ self-assembly. Accordingly, PBP4 has shown to localize to the division septum (Atilano *et al*., 2010).

These observations prove that the system does not work properly in *S.aureus*, and therefore it does not allow us to take further conclusions about PBP2 and PBP4 interactions. Possibly due to improved folding of GFP$_{P7}$, fragments resulting from GFP$_{P7}$ splitting can establish self-interactions, even if proteins to which they are attached do not interact with each other. However, this was not observed in previous studies where enhanced an enhanced version of YFP (eYFP) was used for the same purpose (Hu *et al*., 2002; Soufo and Graumann, 2006; Pazos *et al*., 2013). The fact that fusion proteins were being expressed at high levels, from multi-copy plasmids (except for FtsZ fusions) could also pose a limitation for this system. It is known that when expressed at sufficiently high concentrations, fluorescent protein fragments are able of self-association (Cabantous *et al*., 2005). Although the inducers for expression of fusion proteins were optimized, the ideal would be to express them at the same levels as their endogenous proteins.

Unexpectedly, upon co-expression of C-GFP_{P7} and N-GFP_{P7}-PBP2 fusions (**Fig.3.11B**) fluorescence was detected at the cytoplasm, unlike it was observed when N-GFP_{P7} and N-GFP_{P7}-PBP4 were simultaneously expressed in a cell. We suggest that N-GFP_{P7}-PBP2 fusion protein is being cleaved by cellular mechanisms, leaving N-GFP_{P7} fragment free in the cytoplasm, being able to directly associate with the cytoplasmic C-GFP_{P7} fragment. Therefore, N-terminal and C-terminal fragments associate to restore a functional GFP_{P7}, which justifies the cytoplasmic fluorescence, also detected upon co-expression of C-GFP_{P7} and N-GFP_{P7} fusions (**Fig.3.9E**). This could be confirmed by western blot analysis using a specific anti-GFP_{P7} antibody. Fluorescence does not reflects PBP2 localization but instead GFP_{P7} self-assembly at the cytoplasm.

We have proposed an alternative for this system, using a non-improved version of GFP, GFP_{mut1}. Although due to time constrains we were not able to complete tests with this protein, preliminary data indicated that GFP_{mut1} fragments do not self-associate, suggesting that it can be a powerful tool for the interaction of protein interactions, unlike GFP_{P7}. Moreover, a positive control (as a strain expressing N-GFP-FtsZ and C-GFP-EzrA fusions or both GFP_{mut1} fragments bound to zip-zip domains in a BTH system) is needed to confirm this results.

A similar approach could be used by introducing point mutations in superfast GFP, to decrease the signal of negative control (which expresses split-GFP_{P7} fragments), as reported by previous authors (Zhou *et al*., 2011). Another method could be employed by dividing GFP_{P7} in three small fragments (tripartite GFP) in order to decrease unspecific GFP_{P7} association and reduce background signal (Cabantous *et al*., 2013). Förster Resonance Energy Transfer (FRET) has also been a successful tool for the visualization of protein-protein interactions *in vivo* (Kerppola, 2008). FRET analysis requires the interaction between two fluorophores, fused to putative interacting proteins. The principle of FRET is based on the energy transfer from a donor to an acceptor fluorophore (capable of absorbing the donor energy) when proteins to which they are fused are located in very close proximity (2-10 nm) (Förster, 1948). As FRET requires higher levels of protein expression than BiFC (Kerppola, 2008), the expression of protein fusions from multi-copy plasmids (as employed in our system) is suitable and becomes an advantage for the detection of protein interactions.

In summary, we tested the applicability of a split-GFP_{P7} system to study interactions putative interacting proteins PBP2 and PBP4 in living cells of *S.aureus*. As GFP_{P7} fragments were shown to be able of self-assembly, split-GFP_{P7} system generated false positive results and thereby is a non-reliable method to study protein interactions in this pathogen.

REFERENCES

Adams, D. W. & Errington, J. 2009. Bacterial cell division: assembly, maintenance and disassembly of the Z ring. Nature Reviews Microbiology 7:642–653.

Alaedini, A, & Day, R. A. 1999. Identification of two penicillin-binding multienzyme complexes in Haemophilus influenzae. Biochemical and Biophysical Research Communications 264:191–195.

Atilano, M. L., Pereira, P. M., Yates, J., Reed, P., Veiga, H., Pinho, M. G. & Filipe, S. R.2010. Teichoic acids are temporal and spatial regulators of peptidoglycan cross-linking in Staphylococcus aureus. Proceedings of the National Academy of Sciences of the United States of America 107:18991–18996.

Bartley J. 2002. First case of VRSA identified in Michigan. Infection Control Hospital Epidemiology 23:480.

Bhardwaj, S., & R. A. Day. 1997. Detection of intracellular protein-protein interactions: penicillin interactive proteins and morphogene proteins, *In* Techniques in protein chemistry (D. Marshak ed.), VIII, pp 469–480, Academic Press New York, N.Y.

Buddelmeijer, N. & Beckwith, J. 2004. A complex of the Escherichia coli cell division proteins FtsL, FtsB and FtsQ forms independently of its localization to the septal region. Molecular Microbiology 52:1315–1327.

Cabantous S., Nguyen, H. B., Pedelacq, J., Koraïchi, F., Chaudhary, A., Ganguly, K., Lockard, M. A., Favre, G., Terwilliger, T. C & Waldo, G. S. 2013. A new protein-protein interaction sensor based on tripartite split-GFP association. Scientific Reports 3:2854.

Cabantous, S., Terwilliger, T. C. & Waldo, G. S. 2005. Protein tagging and detection with engineered self-assembling fragments of green fluorescent protein. Nature Biotechnology 23:102–107.

Claessen, D., Emmins, R., Hamoen, L. W., Daniel, R. A., Errington, J. & Edwards, D. H. 2008. Control of the cell elongation-division cycle by shuttling of PBP1 protein in Bacillus subtilis. Molecular Microbiology 68:1029–1046.

Couto, I., De Lencastre, H., Severina, E., Kloos. W, Webster, J. A., Hubner, R. J., Sanches, I. S. & Tomasz, A. 1996. Ubiquitous presence of a mecA homologue in natural isolates of Staphylococcus sciuri. Microbial Drug Resistance 2:377–391.

Cui, L., Murakami, H., Kuwahara-Arai, K., Hanaki, H. & Hiramatsu, K. 2000. Contribution of a thickened cell wall and its glutamine nonamidated component to the vancomycin resistance expressed by Staphylococcus aureus Mu50. Antimicrobial Agents and Chemotherapy 44:2276–2285.

Deleo, F. R. & Chambers, H. F. 2009. Re-emergence of antibiotic-resistant Staphylococcus aureus in the genomics era. Journal of Clinical Investigation 119: 2464-2474.

Deresinski, S. 2007. Counterpoint: Vancomycin and Staphylococcus aureus - an antibiotic enters obsolescence. Clinical Infectious Diseases 44:1543–1548.

Dmitriev, B. A., Toukach, F. V., Schaper, K. -J., Holst, O., Rietschel, E. T. & Ehlers, S. 2003. Tertiary Structure of Bacterial Murein: the Scaffold Model. Journal of Bacteriology 185:3458–3468.

Erickson, H. P. 1997. FtsZ, a tubulin homologue in prokaryote cell division. Trends in Cell Biology 7:362–367.

Erickson, H. P. 2001. The FtsZ protofilament and attachment of ZipA - Structural constraints on the FtsZ power stroke. Current Opinion in Cell Biology 13:55–60.

Errington, J., Daniel, R. A. & Scheffers, D. -J. 2003. Cytokinesis in bacteria. Microbiology and Molecular Biology Reviews 67:52–65.

Feilmeier, B. J., Iseminger, G., Schroeder, D., Webber, H. & Phillips, G. J. 2000. Green fluorescent protein functions as a reporter for protein localization in Escherichia coli. Journal of Bacteriology 18:4068–4076.

Figge, R. M., Divakaruni, A. V. & Gober, J. W. 2004. MreB, the cell shape-determining bacterial actin homologue, co-ordinates cell wall morphogenesis in Caulobacter crescentus. Molecular Microbiology 51:1321–1332.

Fisher, A. C. & DeLisa, M. P. 2008. Laboratory evolution of fast-folding green fluorescent protein using secretory pathway quality control. PLoS ONE, 3:e2351.

Förster, T. 1948. Zwischenmolekulare Energiewanderung und Fluoreszenz (Intermolecular energy migration and fluorescence). Annalen der Physik 2:55–75.

Forsyth, R. A., Haselbeck, J. R. & Ohlsen, L. K. 2002. A genome-wide strategy for the identification of essential genes in Staphylococcus aureus. Molecular Microbiology 43:1387–1400.

Foster, T. J. 2005. Immune evasion by staphylococci. Nature Reviews Microbiology 3:948–958.

Fuda, C. C. S., Fisher, J. F. & Mobashery, S. 2005. β-Lactam resistance in Staphylococcus aureus: The adaptive resistance of a plastic genome. Cellular and Molecular Life Sciences 62:2617–2633.

Gentz, R., Rauscher III, F. J, Abate, C. & Curran, T. 1989. Parallel Association of Fos and Jun Leucine Zippers Juxtaposes DNA Binding Domains. Science 243:1695–1699.

Ghuysen, J. -M. 1991. Serine β-Lactamases and Penicillin-binding proteins. Annual Review of Microbiology 45:37–67.

Gill, S. R., Fouts, D. E., Archer, G. L., Mongodin, E. F., Deboy, R. T., Ravel, J., Paulsen, I. T., Kolonay, J. F., Brinkac, L., Beanan, M., Dodson, R. J, Daugherty, S. C, Madupu, R., Angiuoli, S. V., Durkin, A. S., Haft, D. H., Vamathevan, J., Khouri, H., Utterback, T., Lee, C., Dimitrov, G., Jiang, L., Qin, H., Weidman, J., Tran, K., Kang, K., Hance, I. R., Nelson, K. E. & Fraser, C. M. 2005. Insights on Evolution of Virulence and Resistance from the Complete Genome Analysis of an Early Methicillin-Resistant Staphylococcus aureus Strain and a Biofilm-Producing Methicillin-Resistant Staphylococcus epidermidis Strain. Journal of Bacteriology 187:2426–2438.

Goffin, C. & Ghuysen, J. M. 1998. Multimodular penicillin-binding proteins: an enigmatic family of orthologs and paralogs. Microbiology and Molecular Biology Reviews 62:1079–1093.

Graumman, P. 2012a. Cell division. *In* Bacillus: Cellular and Molecular Biology (Gueiros-Filho, F. ed.), 2nd ed., pp 85-122, Caister Academic Press, University of Freiburg, Germany.

Graumman, P. 2012b. The Cell Wall of Bacillus subtilis. *In* Bacillus: Cellular and Molecular Biology (Scheffers, D. J. ed.), 2nd ed., pp 285-313, Caister Academic Press, University of Freiburg, Germany.

Haeusser, D. P., Schwartz, R. L., Smith, A. M., Oates, M. E. & Levin, P. A. 2004. EzrA prevents aberrant cell division by modulating assembly of the cytoskeletal protein FtsZ. Molecular Microbiology 52:801–814.

Haeusser, D. P., Garza, A. C., Buscher, A. Z., Levin, P. A. 2007. The division inhibitor EzrA contains a seven-residue patch required for maintaining the dynamic nature of the medial FtsZ ring. Journal of Bacteriology 189:9001–9010.

Hale, C. A. & De Boer, P. A. J. 1999. Recruitment of ZipA to the Septal Ring of Escherichia coli Is Dependent on FtsZ and Independent of FtsA. Journal of Bacteriology 181:167–176.

Hartman, B. J. & Tomasz, A. 1984. Low-affinity penicillin-binding protein associated with beta-lactam resistance in Staphylococcus aureus. Journal of Bacteriology 158:513–516.

Heijenoort, J. V. 2001. Formation of the glycan chains in the synthesis of bacterial peptidoglycan. Glycobiology 11:25R–36R.

Höltje, J. V. 1998. Growth of the stress-bearing and shape-maintaining murein sacculus of Escherichia coli. Microbiology and Molecular Biology Reviews 62:181–203.

Höltje, J. V. 1996. A hypothetical holoenzyme involved in the replication of the murein sacculus of Escherichia coli. Microbiology 142:1911–1918.

Howe, R. A., Monk. A., Wootton, M., Walsh, T. R. & Enright, M. C. 2004. Vancomycin Susceptibility within Methicillin-resistant Staphylococcus aureus Lineages. Emerging Infectious Diseases 10:855–857.

Hu, C. D., Chinenov, Y. & Kerppola, T. K. 2002. Visualization of interactions among bZIP and Rel family proteins in living cells using bimolecular fluorescence complementation. Molecular Cell 9:789–798.

Jorge, A. M., Hoiczyk, E., Gomes, J. P. & Pinho, M.G. 2011. EzrA contributes to the regulation of cell size in Staphylococcus aureus. PLoS ONE, 6:e27542.

Katayama, Y., Zhang, H. –Z., Hong, D. & Chambers, H. F. 2003. Jumping the barrier to beta-lactam resistance in Staphylococcus aureus. Journal of Bacteriology 185:5465–5472.

Katayama, Y., Ito, T., & Hiramatsu, K. 2000. A new class of genetic element, staphylococcus cassette chromosome mec, encodes methicillin resistance in Staphylococcus aureus. Antimicrobial Agents and Chemotherapy 44: 1549-1555

Kerppola, T. K. 2008. Bimolecular fluorescence complementation (BiFC) analysis as a probe of protein interactions in living cells. Annual Review of Biophysics, 37:465–487.

Kerppola, T. K. 2006. Visualization of molecular interactions by fluorescence complementation. Nature reviews. Molecular Cell Biology 7:449–456.

Koch, A. & Woeste, S. 1992. Elasticity Of The Sacculus Of Escherichia-coli. Journal of Bacteriology 174:4811–4819.

Kodama, Y. & Hu, C.D. 2012. Bimolecular fluorescence complementation (BiFC): A 5-year update and future perspectives. BioTechniques 53:285–298.

Kraemer, G. R. & Iandolo, J. J. 1990. High-frequency transformation of Staphylococcus aureus by electroporation. Current Microbiology 21:373–376.

De Lencastre, H., Oliveira, D. & Tomasz, A. 2007. Adaptative resistance Staphylococcus aureus. Current Opinion in Microbiology 10:428–435.

Leski, T. A. & Tomasz, A. 2005. Role of Penicillin-Binding Protein 2 (PBP2) in the Antibiotic Susceptibility and Cell Wall Cross-Linking of Staphylococcus aureus. Journal of Bacteriology 2:1815–1824.

Levin, P. A, Kurtser, I. G. & Grossman, A. D. 1999. Identification and characterization of a negative regulator of FtsZ ring formation in Bacillus subtilis. Proceedings of the National Academy of Sciences of the United States of America 96:9642–9647.

Löwe, J. & Amos, L. A. 1998. Crystal structure of the bacterial cell-division protein FtsZ. Nature 391:203–206.

Lutkenhaus, J. & Addinall, S. G. 1997. Bacterial cell division and the Z ring. Annual Review of Biochemistry 66:93–116.

Lutkenhaus, J., Pichoff, S. & Du, S. 2012. Bacterial cytokinesis: from Z ring to divisome. Cytoskeleton (Hoboken) 69:778–790.

Memmi, G., Filipe, S. R., Pinho, M. G., Fu, Z., Cheung, A. 2008. Staphylococcus aureus PBP4 is essential for β-lactam resistance in community-acquired methicillin-resistant strains. Antimicrobial Agents and Chemotherapy 52:3955–3966.

Monk, I. R., Shah, I. M. & Xu, M. 2012. Transforming the Untransformable : Application of Direct Transformation To Manipulate Genetically Staphylococcus aureus and Staphylococcus epidermidis. mBio, 3:e00277–11.

Monteiro, J. M., Fernandes, P.B., Vaz, F., Pereira, A. R., Tavares, A. C., Ferreira, M. T., Pereira, P. M., Veiga, H., Kuru, E., VanNieuwenhze, M. S., Brun, Y. V., Filipe, S. R. & Pinho, M. G. 2015. Cell shape dynamics during the staphylococcal cell cycle. Nature Communications 6:8055.

Murakami, K., Fujimura, T. & Doi, M. 1994. Nucleotide sequence of the structural gene for the penicillin-binding protein 2 of Staphylococcus aureus and the presence of a homologous gene in other staphylococci. FEMS Microbiology Letters, 117:131–136.

Navratna, V., Nadig, S., Sood, V., Prasad, K., Arakere, G. & Gopal, B. 2010. Molecular basis for the role of Staphylococcus aureus penicillin binding protein 4 in antimicrobial resistance. Journal of Bacteriology 192:134–144.

Okonog, K., Noji, Y., Nakao, M. & Imada, A. 1995. The possible physiological roles of penicillin-binding proteins of methicillin-susceptible and methicillin-resistantStaphylococcus aureus. Journal of Infection and Chemotherapy 1:50–58.

Okuma, K., Kozue, I., Turnidge, J. D., Grubb, W. B., Bell, J. M., O'Brien, F. G., Coombs, G. W., Pearman, J. W., Tenover, F. C., Kapi, M., Tiensasitorn, C., Ito, T. & Hiramatsu, K. 2002. Dissemination of New Methicillin-Resistant Staphylococcus aureus Clones in the Community. Journal of Clinical Microbiology 40: 4289-4294.

Oshida, T. & Tomasz, A. 1992. Isolation and characterization of a Tn551-autolysis mutant of Staphylococcus aureus. Journal of Bacteriology 174:4952–4959.

Pazos, M., Natale, P., Margolin, W. & Vicente, M. 2013. Interactions among the early Escherichia coli divisome proteins revealed by bimolecular fluorescence complementation. Environmental Microbiology 15:3282–3291.

Pereira, P. M.,Veiga, H., Jorge, A. M. & Pinho, M. G. 2010. Fluorescent reporters for studies of cellular localization of proteins in Staphylococcus aureus. Applied and Environmental Microbiology 76:4346–4353.

Pereira, S. F. F., Henriques, A. O., Pinho, M. G., De Lencastre, H., Tomasz, A. 2009. Evidence for a dual role of PBP1 in cell division and cell separation. Molecular Microbiology 72:895–904.

Pereira, S. F. F, Henriques, A. O., Pinho, M. G., De Lencastre, H. & Tomasz, A. 2007. Role of PBP1 in cell division of Staphylococcus aureus. Journal of Bacteriology 189: 3525–3531.

Pichoff, S., Shen, B., Sullivan, B. & Lutkenhaus, J. 2012. FtsA mutants impaired for self-interaction bypass ZipA suggesting a model in which FtsA's self-interaction competes with its ability to recruit downstream division proteins. Molecular Microbiology 83:151–167.

Pichoff, S. & Lutkenhaus, J. 2002. Unique and overlapping roles for ZipA and FtsA in septal ring assembly in Escherichia coli. European Molecular Biology Organization 21:685–693.

Pinho, M. G., Filipe, S. R. De Lencastre, H., Tomasz, A. 2001b. Complementation of the essential peptidoglycan transpeptidase function of penicillin-binding protein 2 (PBP2) by the drug resistance protein PBP2A in Staphylococcus aureus. Journal of Bacteriology 183:6525–6531.

Pinho, M. G. & Errington, J. 2003. Dispersed mode of Staphylococcus aureus cell wall synthesis in the absence of the division machinery. Molecular Microbiology 50:871–881.

Pinho, M. G. & Errington, J. 2005. Recruitment of penicillin-binding protein PBP2 to the division site of Staphylococcus aureus is dependent on its transpeptidation substrates. Molecular Microbiology 55:799–807.

Pinho, M. G., Kjos, M. & Veening, J. -W. 2013. How to get (a)round: mechanisms controlling growth and division of coccoid bacteria. Nature Reviews Microbiology 11:601–14.

Pinho, M. G., De Lencastre, H. & Tomasz, A. 2000. Cloning, characterization, and inactivation of the gene pbpC, encoding penicillin-binding protein 3 of Staphylococcus aureus. Journal of Bacteriology 182:1074–1079.

Pinho, M.G., Lencastre, H. & Tomasz, A., 2001a. An acquired and a native penicillin-binding protein cooperate in building the cell wall of drug-resistant staphylococci. Proceedings of the National Academy of Sciences of the United States of America 98:10886–10891.

Reed, P., Atilano, M.L., Alves, R., Hoiczyk, E., Sher, X., Reichmann, N. T., Pereira, P. M., Roemer, T., Filipe, S. R., Pereira-Leal, J. B., Ligoxygakis, P. & Pinho, M. G. 2015. Staphylococcus aureus Survives with a Minimal Peptidoglycan Synthesis Machine but Sacrifices Virulence and Antibiotic Resistance. PLOS Pathogens 11:e1004891.

Rowland, S. L., Wadsworth, K. D., Robson, S. A., Robichon, C., Beckwith, J. & King, G. F. 2010. Evidence from artificial septal targeting and site-directed mutagenesis that residues in the extracytoplasmic β-domain of DivIB mediate its interaction with the divisomal transpeptidase PBP2B. Journal of Bacteriology 192:6116–6125.

Sambrook, J., E. F. Fritsch, and T. Maniatis. 1989. *In* Molecular cloning: a laboratory manual, 2nd ed., Cold Spring Harbor Laboratory Press, Cold Spring Harbor, N.Y.

Scheffers, D. & Errington, J. 2004. PBP1 Is a Component of the Bacillus subtilis Cell Division Machinery. Society 186:5153–5156.

Scheffers, D. & Pinho, M. 2005. Bacterial cell wall synthesis: new insights from localization studies. Microbiology and Molecular Biology Reviews 69:585–607.

Schleifer, K. H. & Kandler, O. 1972. Peptidoglycan types of bacterial cell walls and their taxonomic implications. Bacteriological Reviews 36:407–477.

Shaner, N. C., Patterson, G. H. & Davidson, M. W. 2007. Advances in fluorescent protein technology. Journal of Cell Science 120:4247–4260.

Shore, A. C. & Coleman, D. C. 2013. Staphylococcal cassette chromosome mec: Recent advances and new insights. International Journal of Medical Microbiology 303:350–359.

Sieradzki, K., Pinho, M. G. & Tomasz, A. 1999. Inactivated pbp4 in Highly Glycopeptide-resistant Laboratory Mutants of Staphylococcus aureus. The Journal of Biological Chemistry 274:18942–18946.

Sieradzki, K. & Tomasz, A. 1999. Gradual alterations in cell wall structure and metabolism in vancomycin-resistant mutants of Staphylococcus aureus. Journal of Bacteriology 181:7566–7570.

Sieradzki, K. & Tomasz, A. 1997. Suppression of β-lactam antibiotic resistance in a methicillin-resistant Staphylococcus aureus through synergic action of early cell wall inhibitors and some other antibiotics. Journal of Antimicrobial Chemotherapy, 39:47–51.

Simon, M. J. & Day, R. A. 2000. Improved Resolution of Hydrophobic Penicillin-binding Proteins and Their Covalently Linked Complexes on a Modified C18 Reversed Phase Column. Analytical Letters 33:861–867.

Soufo, H. J. D. & Graumann, P. L. 2006. Dynamic localization and interaction with other Bacillus subtilis actin-like proteins are important for the function of MreB. Molecular Microbiology 62:1340–1356.

Steele, V. R., Bottomley, A. L., Garcia-Lara, J., Kasturiarachchi, J., Foster, S. J. 2011. Multiple essential roles for EzrA in cell division of Staphylococcus aureus. Molecular Microbiology 80:542–555.

Tavares, J. R., De Souza, R. F., Meira, G. L. S., Gueiros-Filho, F. J. 2008. Cytological characterization of YpsB, a novel component of the Bacillus subtilis divisome. Journal of Bacteriology 190:7096–7107.

Typas, A., Banzhaf, M., Gross, C. A. & Vollmer, W. 2012. From the regulation of peptidoglycan synthesis to bacterial growth and morphology. Nature Reviews Microbiology 10:123–136.

Udo, E. E., Pearman, J. W. & Grubb, W. B. 1993. Genetic analysis of community isolates of methicillin-resistant Staphylococcus aureus in Western Australia. Journal of Hospital Infection 25:97–108.

Vollmer, W. & Bertsche, U., 2008. Murein (Peptidoglycan) structure, architecture and biosynthesis in Escherichia coli. Biochimica et Biophysica Acta - Biomembranes 1778: 1714–1734.

Vollmer, W., Höltje, J. & Ho, J. 2004. The Architecture of the Murein (Peptidoglycan) in Gram-Negative Bacteria: Vertical Scaffold or Horizontal Layer (s)?. Journal of Bacteriology 186:5978–5987.

Voyich, J. M, Braughton, K. R, Sturdevant, D. E., Whitney, A. R., Saïd-Salim, B., Porcella, S. F., Long, R. D., Dorward, D. W., Gardner, D. J., Kreiswirth, B. N., Musser, J. M. & DeLeo, F. R. 2005. Insights into mechanisms used by Staphylococcus aureus to avoid destruction by human neutrophils. Journal of Immunology 175:3907–3919.

Wada, A. & Watanabe, H. 1998. Penicillin-binding protein 1 of Staphylococcus aureus is essential for growth. Journal of Bacteriology 180:2759–2765.

Walsh, T. R. & Howe, R. A. 2002. The prevalence and mechanisms of vancomycin resistance in Staphylococcus aureus. Annual Review of Microbiology 56:657–675.

Wardenburg, J. B., Palazzolo-Ballance, A. M, Otto, M., Schneewind, O. & Deleo, F. R. 2008. Panton-Valentine leukocidin is not a virulence determinant in murine models of community-associated methicillin-resistant Staphylococcus aureus disease. Journal of Infectious Diseases 198:1166–1170.

Weiss, D. S. 2004. Bacterial cell division and the septal ring. Molecular Microbiology 54:588–597.

Wyke, A. W., Ward, J. B., Hayes, M. V. & Curtis, N. A. 1981. A role in vivo for penicillin-binding protein-4 of Staphylococcus aureus. European Journal of Biochemistry 119:389–393.

Yu, Y. & Lutz, S. 2011. Circular permutation: A different way to engineer enzyme structure and function. Trends in Biotechnology 29:18–25.

Zhou, J., Lin, J., Zhou, C., Deng, X. & Xia, B. 2011. An improved bimolecular fluorescence complementation tool based on superfolder green fluorescent protein. Acta Biochimica et Biophysica Sinica 43:239–244.

APPENDIX

Table A.1 DNA fragments expected sizes (kb) from restriction digestion of inserts

	FtsZ-C-GFP_{P7}	FtsZ-N-GFP_{P7}	EzrA-C-GFP_{P7}	EzrA-N-GFP_{P7}	PBP4-C-GFP_{P7}	N-GFP_{P7}-PBP2
BamHI/ EcoRI			0.29 kb	0.50 kb	0.29 kb	
BglII/EagI			1.26 kb	1.26 kb	linearized	
NdeI			undigested	linearized	1.2 kb	
BamHI	2.13 kb	2.13 kb				
NcoI	linearized	2.33 kb				
BamHI/ NcoI	2.31 kb + 2.13 kb	2.33 kb + 2.13 kb + 0.19 kb				
EcoRI						2.04 kb

Note: BamHI/ EcoRI restriction enzymes were used to check for *n-gfp*$_{p7}$ and *c-gfp*$_{p7}$ in EzrA and PBP4 fusions. BglII/EagI restriction enzymes were used to confirm *ezrA* in EzrA fusions. NdeI was used to confirm *pbp4* in PBP4 fusions. BamHI was used to check for *ftsZ* in FtsZ fusions. NcoI was used to check for *n-gfp*$_{p7}$ and *c-gfp*$_{p7}$ in FtsZ fusions.